Can invasive methods of embryo genetic testing be replaced by non-invasive methods in IVF clinics?

From: Minimally Invasive Cell-Free Human Embryo Aneuploidy Testing (miPGT-A) Utilizing Combined Spent Embryo Culture Medium and Blastocoel Fluid – Towards Development of a Clinical Assay

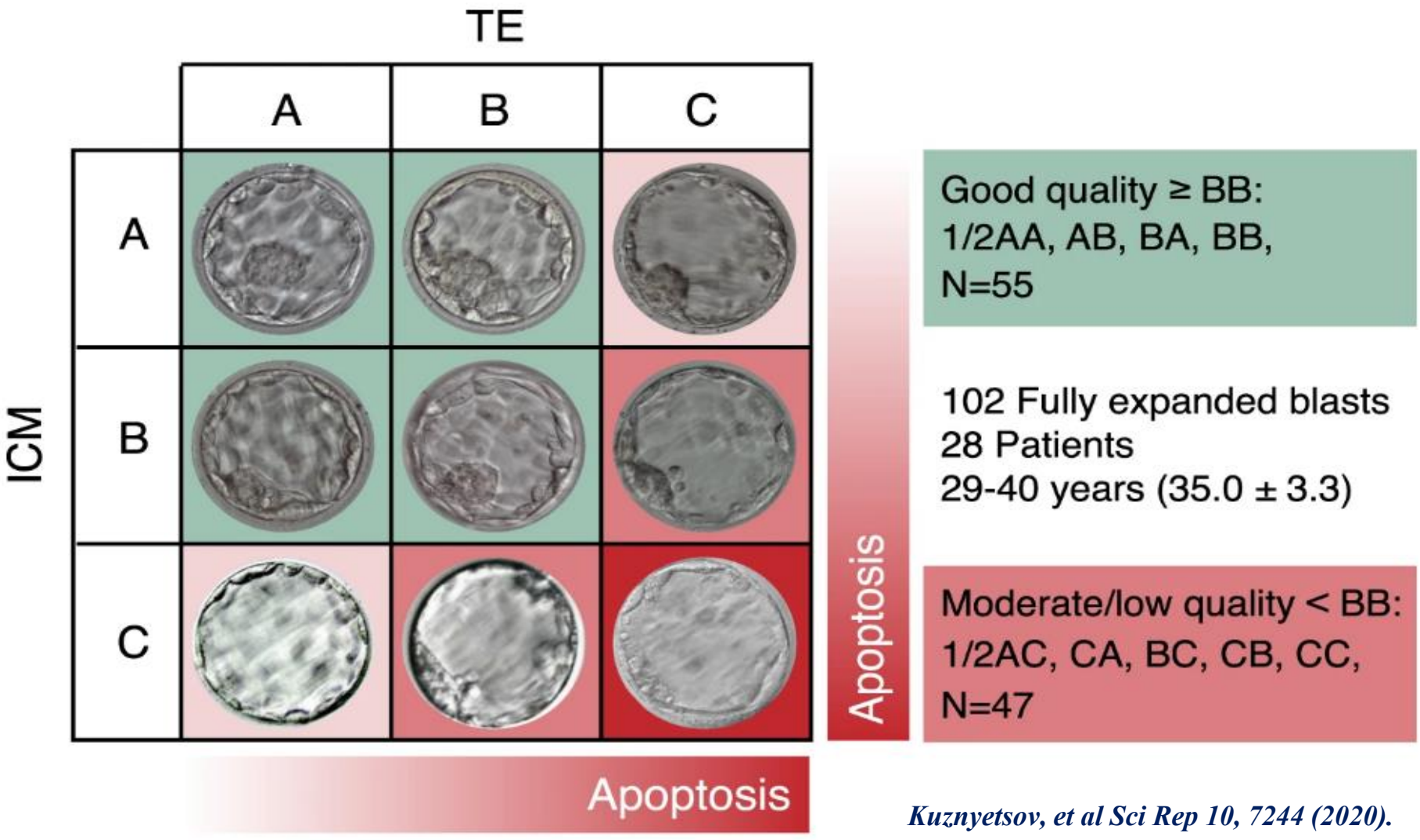

Kuznyetsov, et al Sci Rep 10, 7244 (2020).

Modified SART grading (Heitmann et al, 2013)[50]

Simplified morphological scoring of blastocyst categorized them into two groups: good quality (≥BB) and moderate/low quality (<BB). The rate of apoptotic events is higher in lower morphologic grade embryos.

PGT-A – The concept

Standard embryo evaluations do not reveal embryos with the wrong number of chromosomes

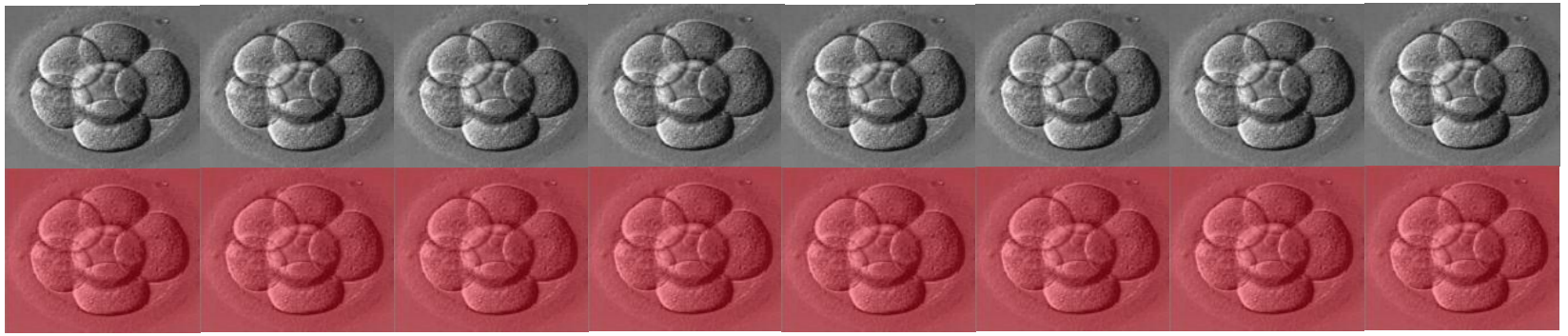

Ideally, one embryo is transferred to the uterus

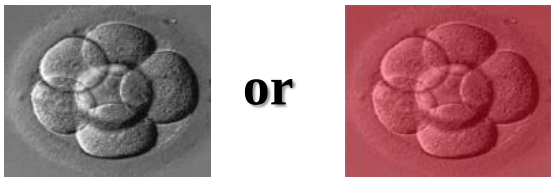

or

after chromosome screening

Munne et al., 1993

Genetic Assessment……

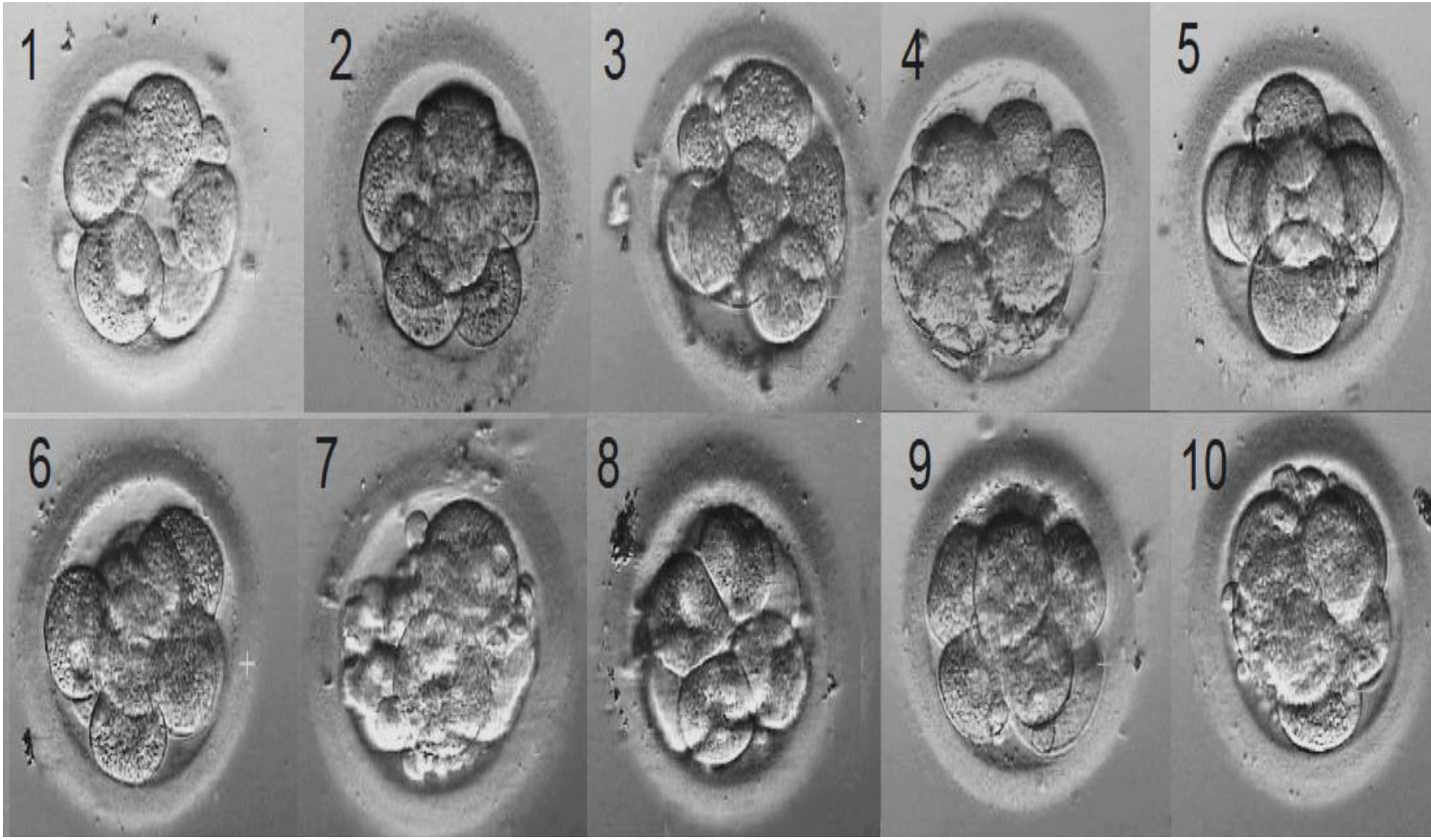

Genetic Assessment……

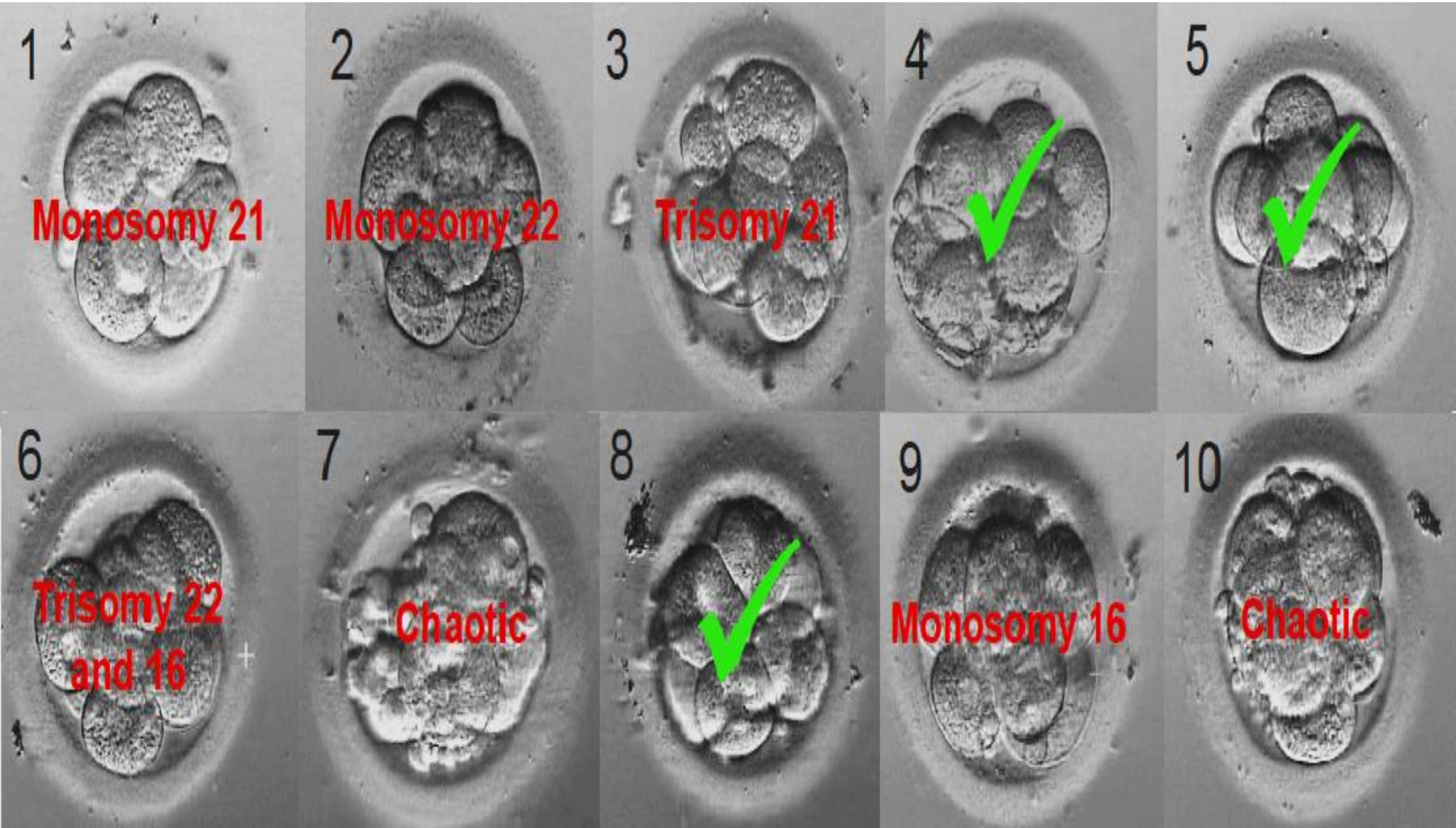

Prenatal and postnatal outcome of mosaic embryo transfers:

multicentric study of one thousand mosaic embryos diagnosed by preimplantation genetic testing with trophectoderm biopsy

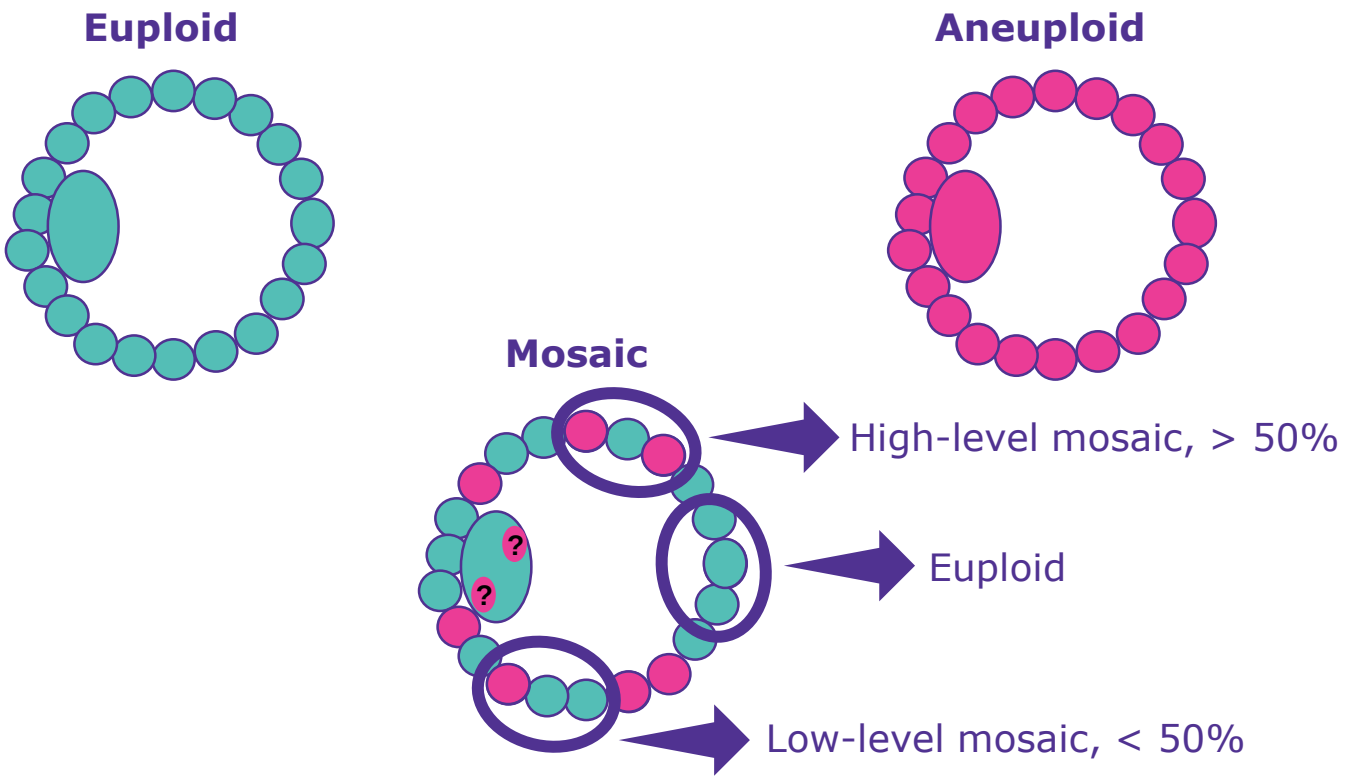

Spinella F, et al. Presented at ESHRE 2021; O-201.

Factors that may affect the outcome of PGT

- Biopsy
- Removal of ‘excluded’ cells
- Artefacts on amplification
- Accumulation of aneuploid cells in the TE

ESHRE PGT-SR/PGT-A Working Group. Hum Reprod Open.2020;3:hoaa017,

Prenatal diagnostic testing

- 465 embryos implanted
- 20% abortion rate
- 3 stillbirths
- Prenatal diagnostic testing

in >200 **pregnancies:**

- 98% normal
- 2% abnormal

CASE	PGT-A results	Amniocentesis results	Outcome	Birth
#884	Whole Chr17 loss, 30%	Unrelated balanced translocation	Birth	Healthy
#1028	Whole Chr9 loss, 34%	Paternal balanced translocation	Birth	Healthy
#865	Whole Chr2, Chr8 loss, 30%	Unrelated interstitial microdeletion Chr2q13, 84 kb	Birth	Healthy
#772	5p gain, 36%	Benign unrelated deletion below the resolution of NGS, maternally inherited	Birth	Healthy
#734	13q gain, 31%	Benign unrelated duplication below the resolution of NGS maternally inherited	Birth	Healthy
#1061	del12p, 8 Mb, 35%	Benign unrelated Chr12 duplication, 2 Mb	Birth	Healthy
#893	Chr16p gain, 34%	Benign unrelated microdeletion	Birth	Healthy
#785	5p gain, 37%	Unrelated deletion below the resolution of NGS, maternally inherited	Ongoing	
#753	14q loss, 29%	Mosaicism and uniparental disomy of a different chromosome	Late abortion	

0% of prenatal diagnostic tests reflected the PGT-A result

Spinella F, et al. Presented at ESHRE 2021; O-201.

Pregnancy outcome

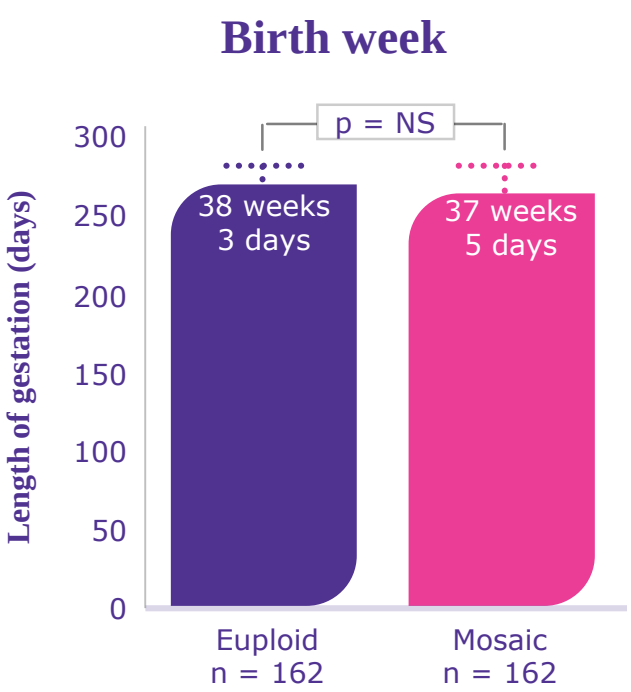

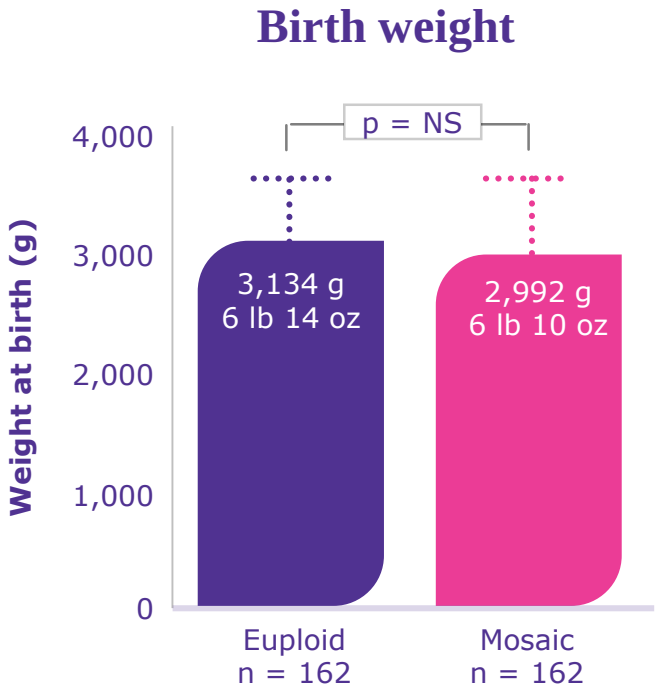

Spinella F, et al. Presented at ESHRE 2021; O-201.

Summary

- Mosaics could not be detected during prenatal diagnostic testing
- Pregnancy duration and birth weight of children are comparable
- Standard postnatal medical examinations revealed no abnormalities
  - Longer follow-up needed
- Live birth rate lower in mosaic embryos

Transfer of (low-level) mosaic embryos may be considered

Spinella F, et al. Presented at ESHRE 2021; O-201.

Pregnancy rate after mosaic transfer relative to the mosaic

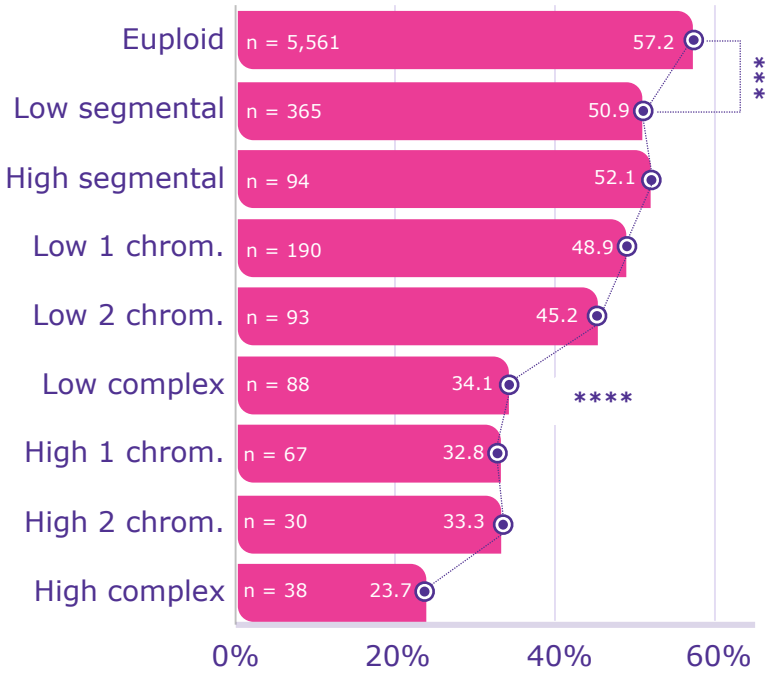

Implantation

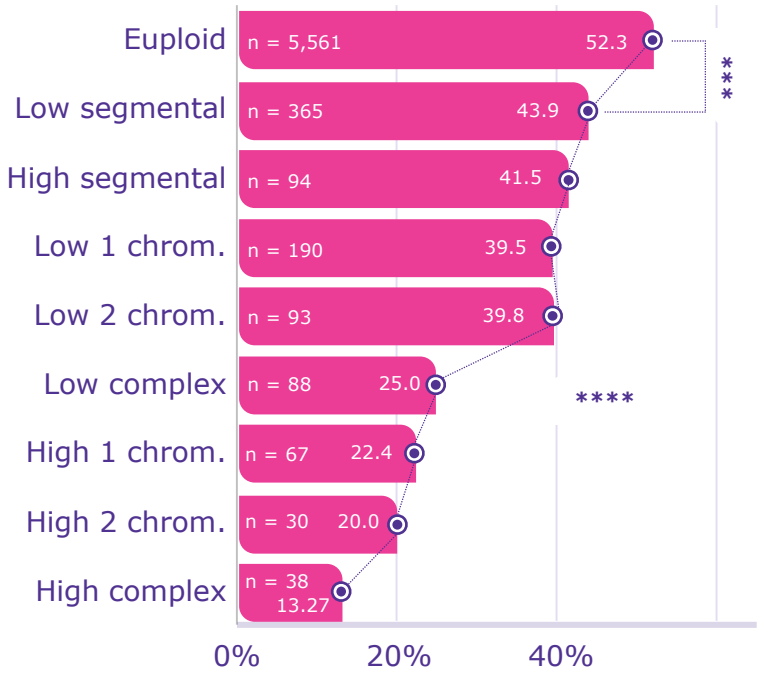

Ongoing PR/LBR

Viotti M, et al. Fertil Steril. 2021;115:1212-24.

Conclusion for practice: mosaic embryos

- 1st choice for euploid embryo transfer
- Do not transfer aneuploid embryos
- Do not discard mosaic embryos, but consider for transfer depending on diagnosis (< or > 50% mosaic)
- Intensive discussion with couple

CoGEN Statement. IVF Worldwide. Available at: https://ivf-worldwide.com/cogen/general/cogen-statement.html. Accessed August 2021.

Prioritization of mosaics

1. Trisomies 13, 18, 21, 22 – viable trisomies
2. Trisomies 14, 15 – associated with uniparental disomy
3. Trisomies 2, 7, 16 – associated with growth retardation
4. All other trisomies

Monosomies may be regarded in the same way as trisomies

[a] Transfer of mosaic embryos with "viable" aneuploidies should be considered with extreme caution.

Preimplantation Genetic Diagnosis International Society (PGDIS). Reprod Biomed Online. 2008;16:134-47.
CoGEN Statement. IVF Worldwide. Available at: https://ivf-worldwide.com/cogen/general/cogen-statement.html. Accessed August 2021.

Impact of embryologist

Is mosaicism affected by an embryologist's experience in biopsy?

- **13 embryologists competent to perform TE biopsy**
  - Group A (n = 5): > 1 year biopsy experience
  - Group B (n = 8): < 1 year biopsy experience
- **Blastocyst**
  - Day 5, 6 and 7 blastocysts (According to Gardner's Grading System)
  - Study period: Jan 2018 – Dec 2019 in Alpha IVF
- **Biopsy method**
  - Either laser + pulling/flicking method or both
  - Generally 5–10 TE cells biopsied

Yap WY, et al. Presented at ESHRE 2021; O-204.

Higher mosaic rate in group of new embryologists

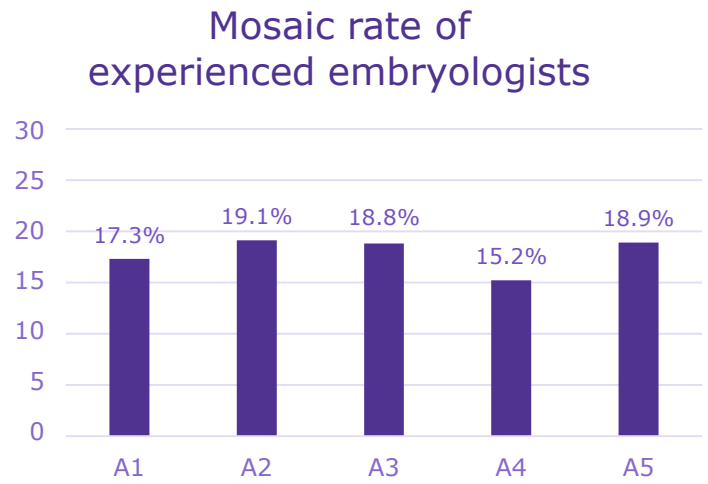

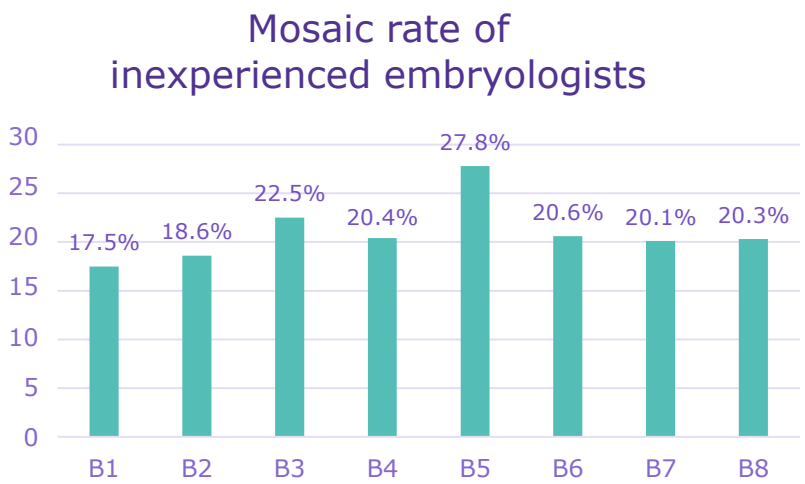

Yap WY, et al. Presented at ESHRE 2021; O-204.

Stage-Appropriateness

DAY 3

Slow „Normal“ Fast

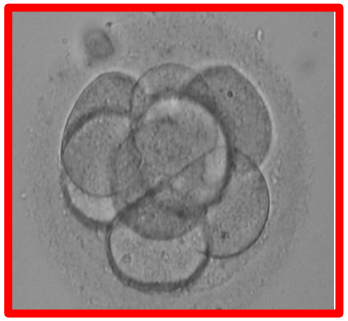

DAY 4

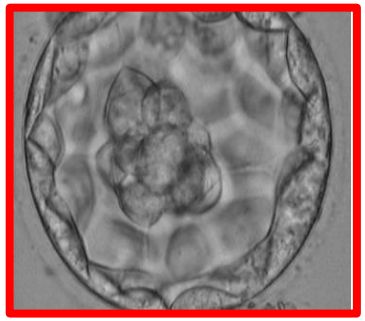

Time-Lapse

What is it all about ?

Fundamentals of Human Embryo Development

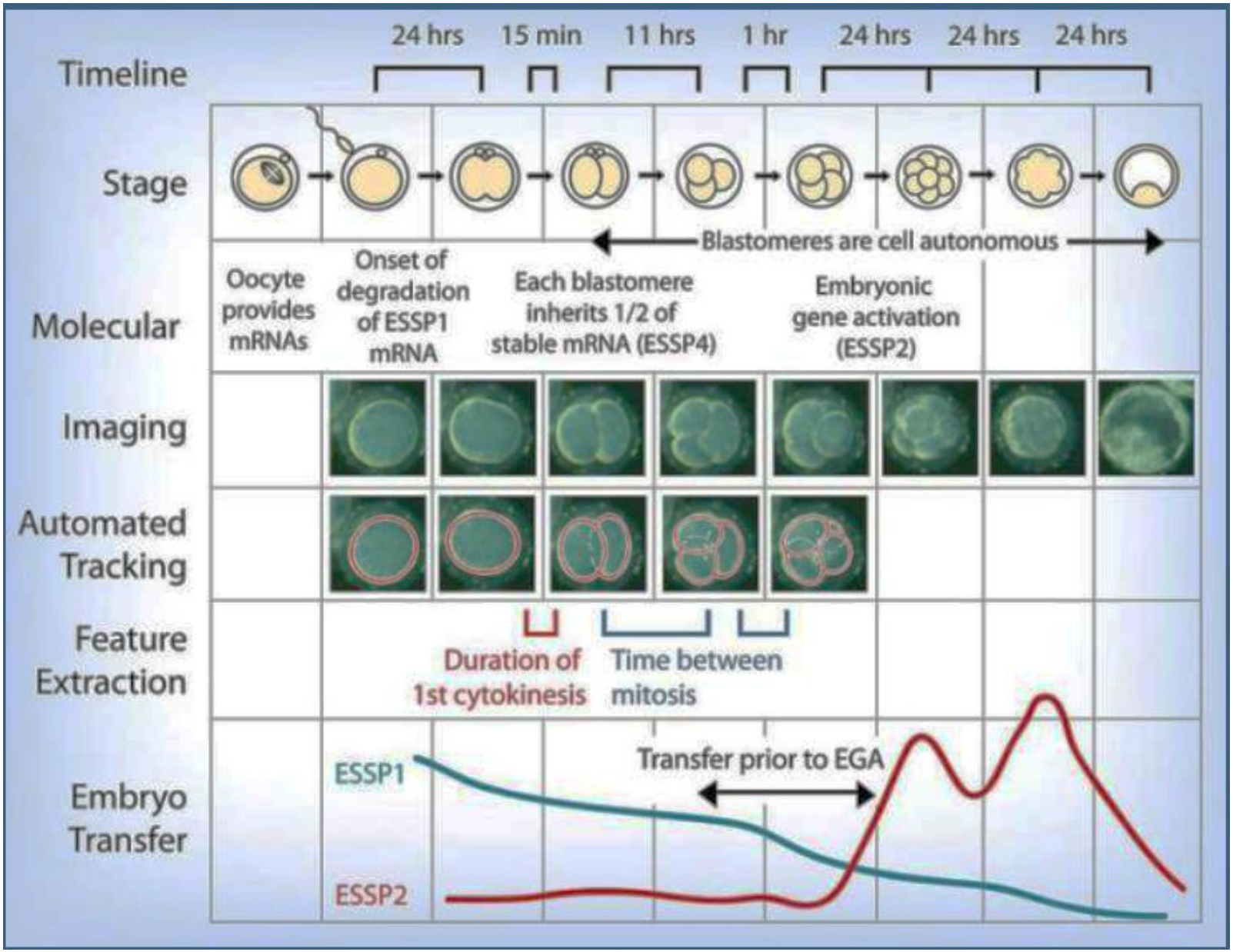

Wong et al; Nature Biotechnology, 2010

Morphology and growth kinetics

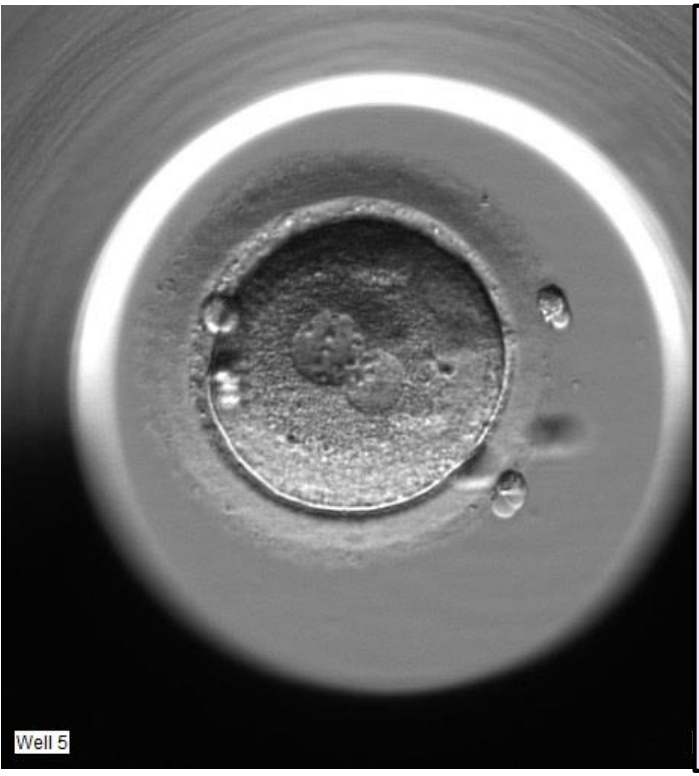

- Timeline of development
- Time between major events
- Detect strange events

–1 ➡ 3 cleavage

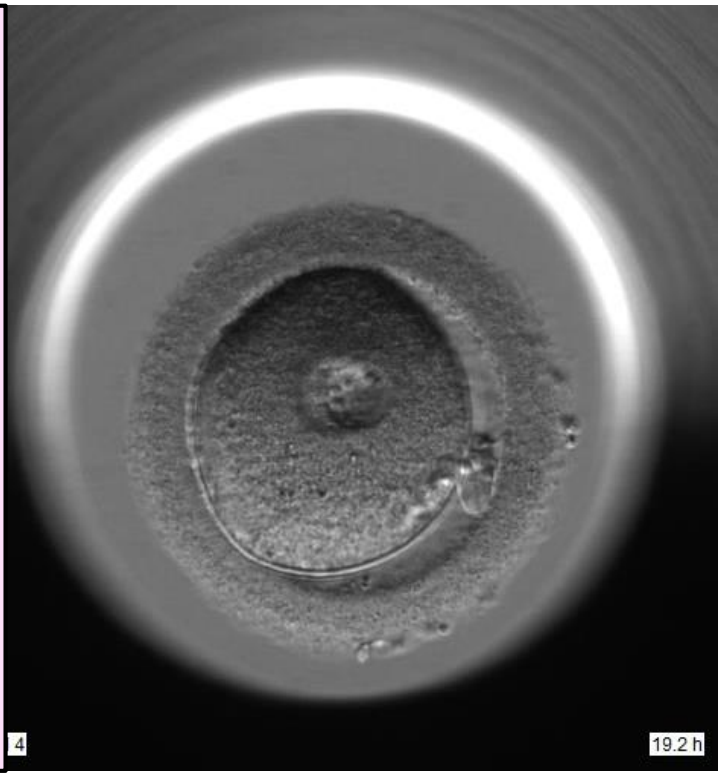

Morphokinetic identification of cell cycles: t2,t3,t4,t5,cc2,s2

t2 :1st.cell division
cc1 :1st.cell cycle
s1 :1st.syncrony

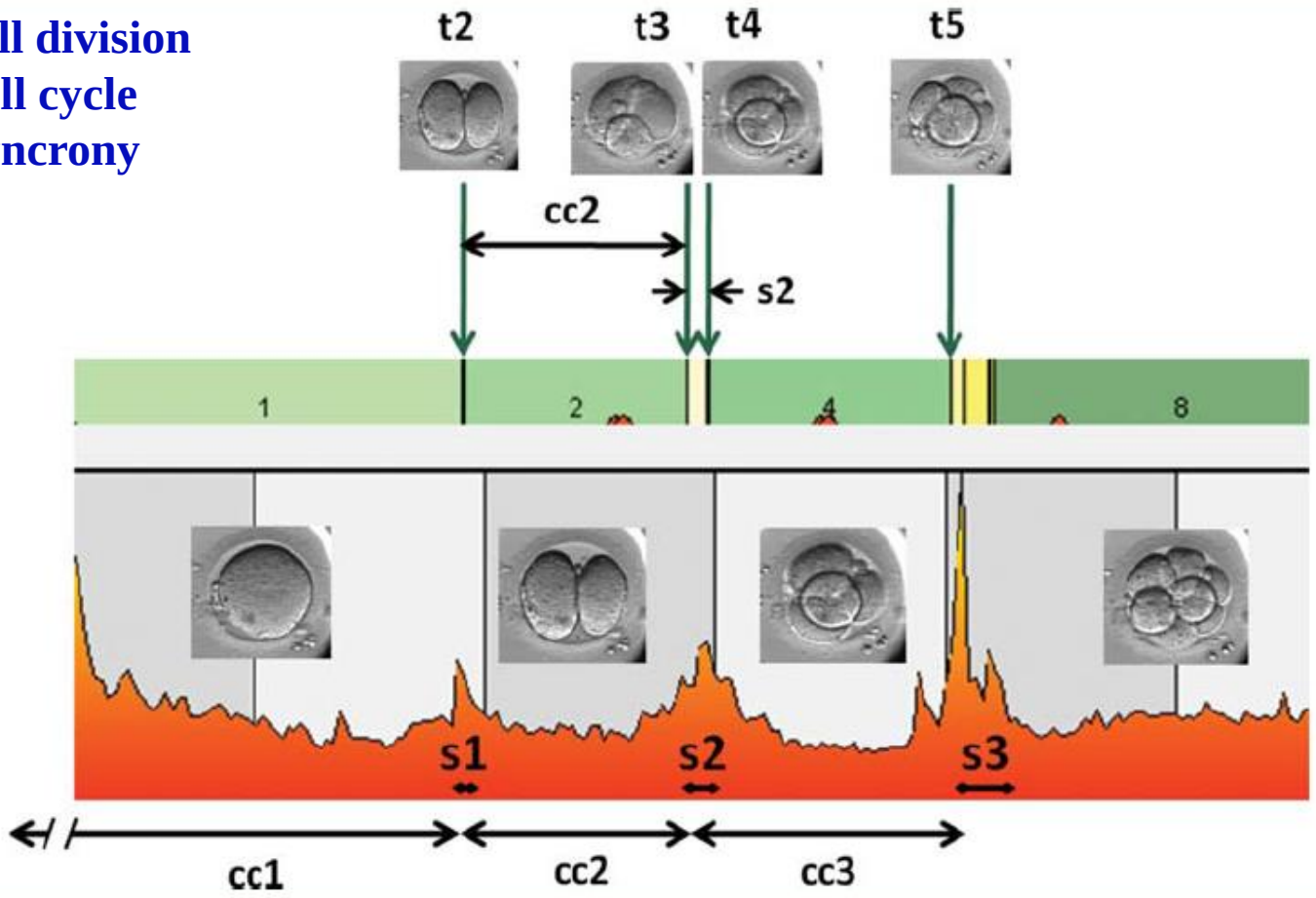

Figure 1 Graphic representation of the considered embryo developmental events t2, t3, t4, t5, cc2 = t3-t2 and s2 = t4-t3. We identified the precise timings and measured them in hours post ICSI microinjection.

Correlation between time taken to reach each development milestrone and the implantation potential of each embryo

Meseguer et al.,HR 2011

Time-lapse markers used for clinical outcome predictions

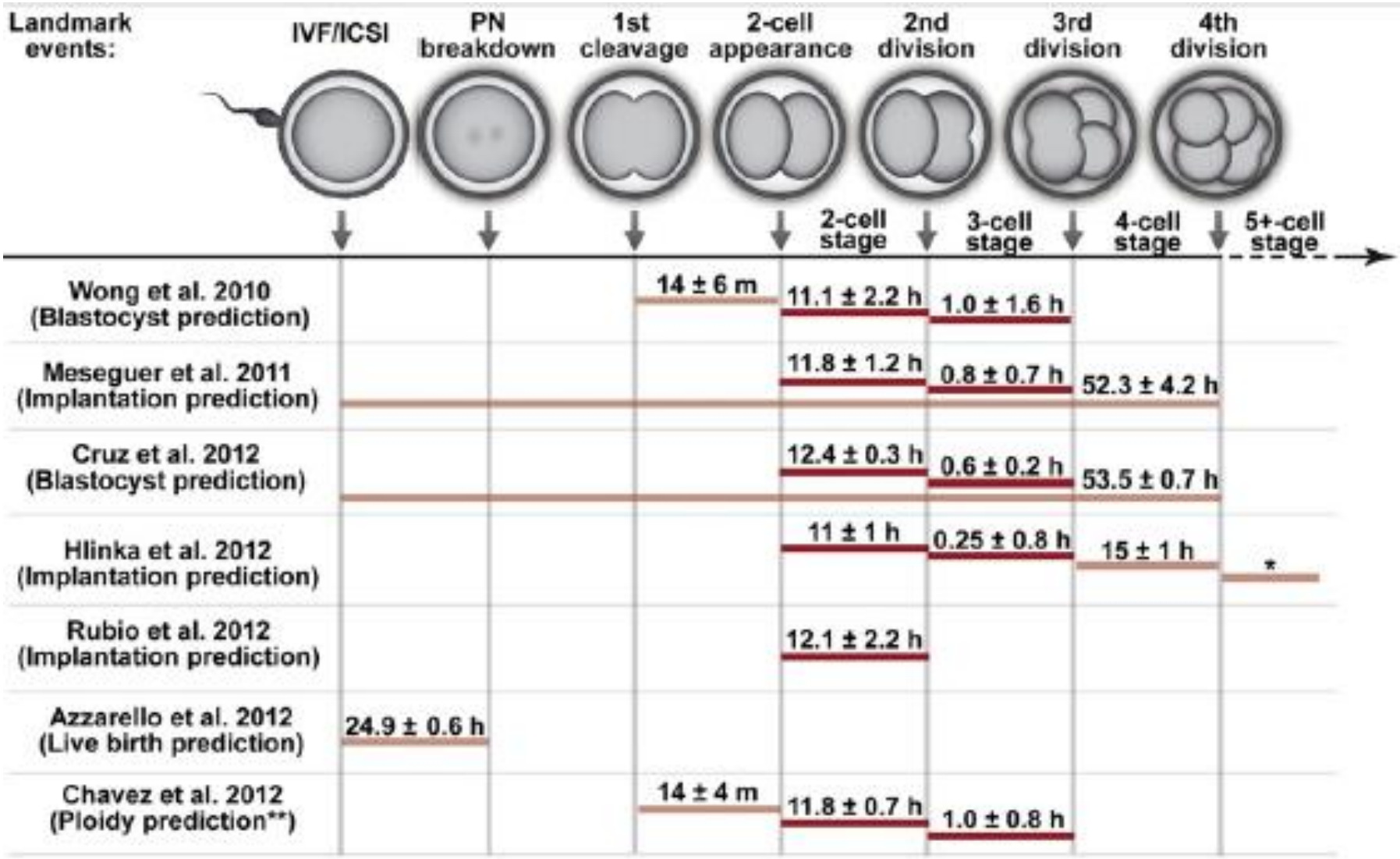

* 5-8 cell stage: 40 ± 10 m; 8 cell stage: 23 ± 1 h; 9-16 cell stage: 55 ± 15 m

** dynamic assessment of fragmentation was also included in the study

Chen et al.,F&S 2013

MORPHOKINETICS

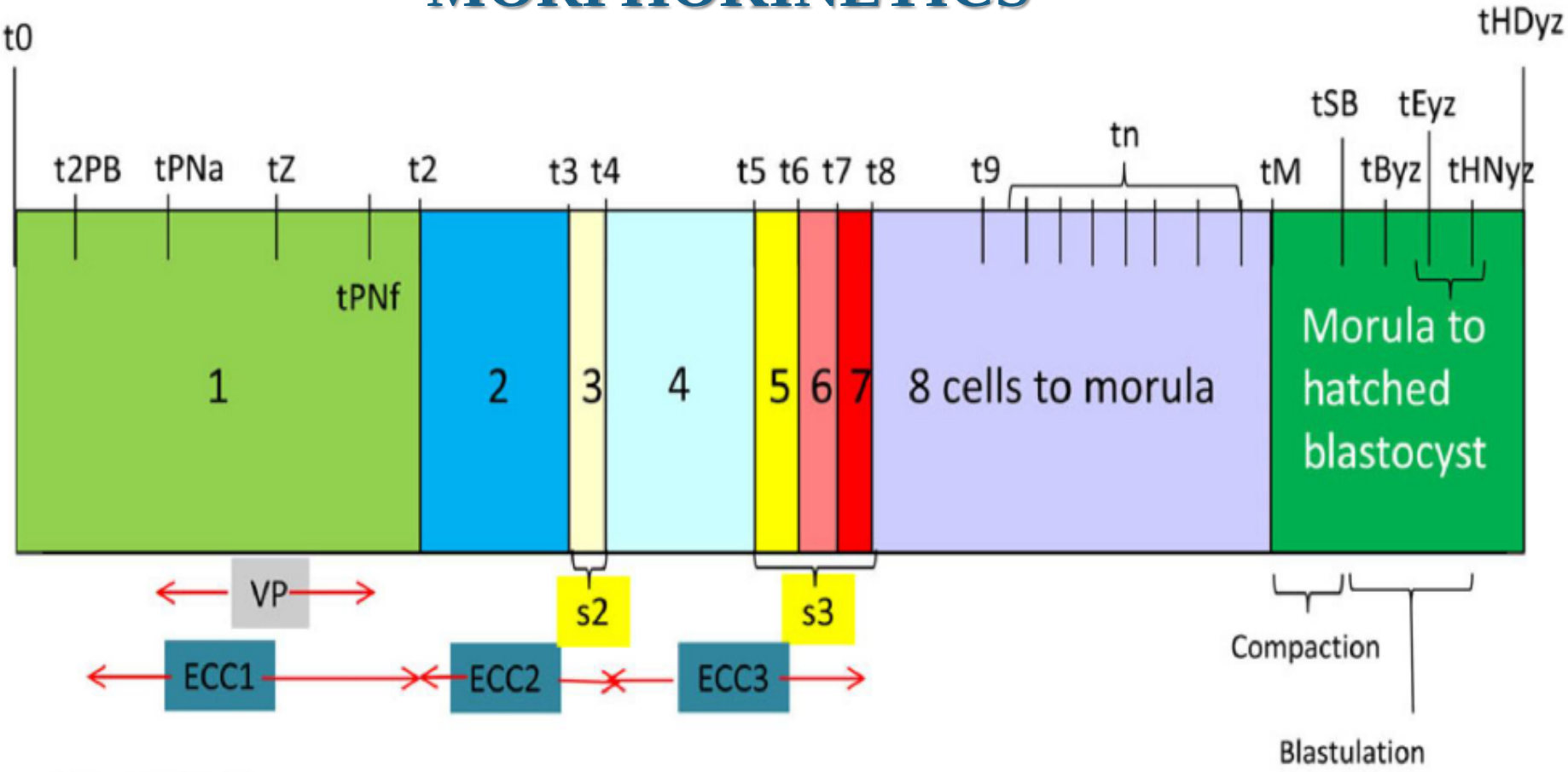

VP = tPNf-tPNa
ECC1 = t2 – tPB2
ECC2 = t4 - t2
ECC3 = t8 - t4
s2 = t4 - t3
s3 = t8 - t5

Compaction = tM - tSC
Blastulation = tB– tSB

Ciray et al., HR 2014

- ✓ *Duration of cell cycles*
- ✓ *Synchronization*

Timelapse to identify chromosomally abnormal embryos?

- **Timelapse is not useful**:

–Kramer et al.

JARG (2014)

–Deven et al.

J. Hum. Reprod. Sci. (2016)

- **Timelapse is useful**:

–Minasi et al.

Hum. Reprod (2016)

–Basile et al.

Fertil Steril (2014)

–Carme Nogales et .al.

Fertil Steril (2017)

–Chawla et a.

JARG (2015)

–Campell at al.

RBM Online (2013)

–Shawn et al.

Nat. Comm. (2012)

Viability assessment by birefringence imaging with polarization microscopy

Spindle imaging of the MII oocyte

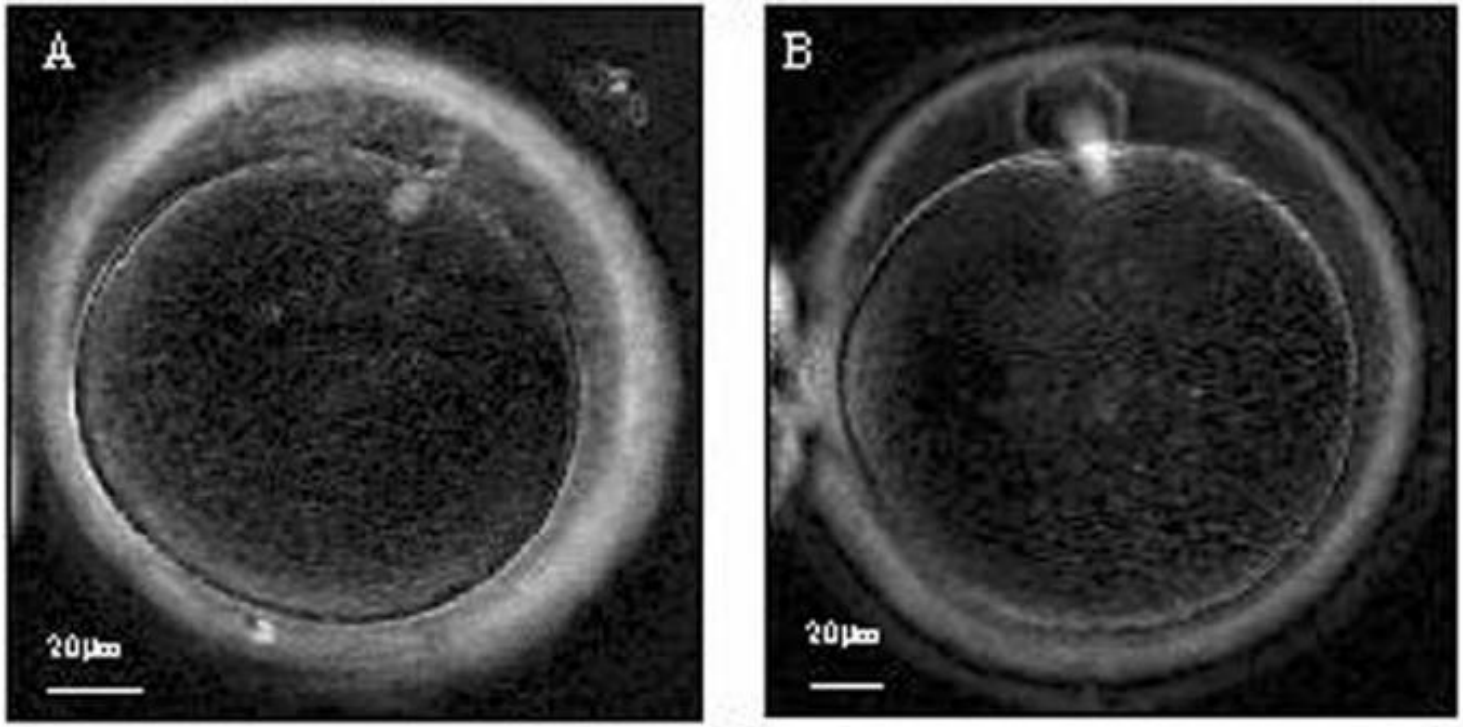

Figure 1. Human oocytes with an extruded PBI showing (**A**) a fully formed MII spindle and (**B**) a spindle in which chromosome segregation has not been completed.

De Santis et al., RBM Online 2005

During meiosis and fertilization meiotic spindles are responsible for proper segregation of the nuclear material, and abnormalities in this fragile structure can lead to infertility, miscarriage and genetic diseases, such as Down syndrome

Oocyte zona birefringence intensity

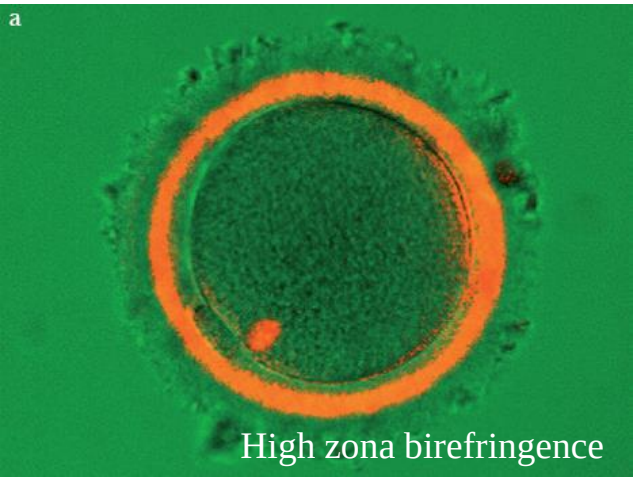

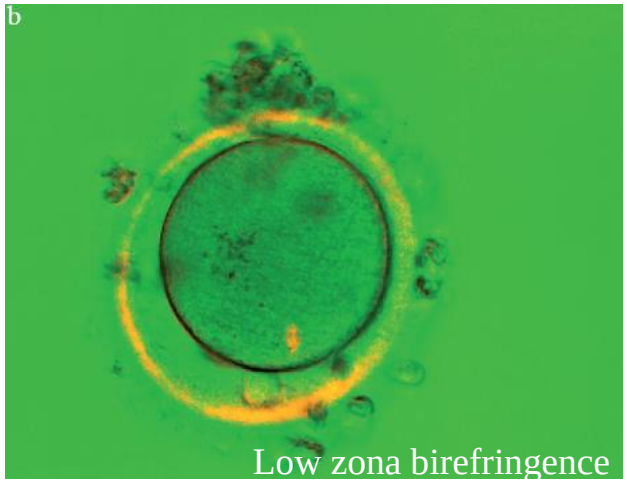

Montag et al.,RBM Online 2008

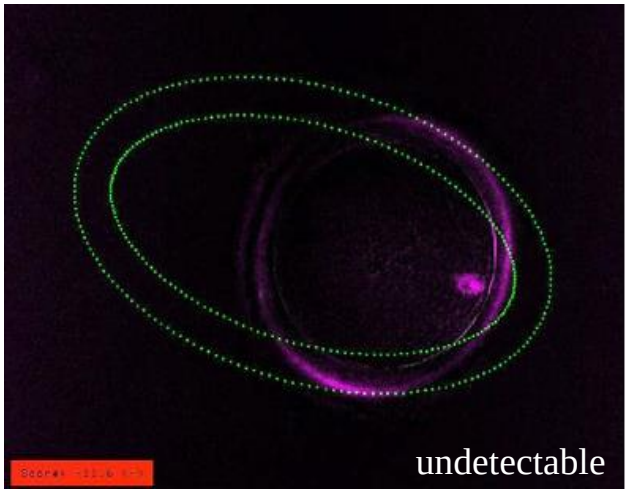

Ebner-Balaban F&S 2010

Polarization microscopy allows the distinction of three layers within the ZP. Inner layer exhibits the highest birefringence(Pelletier 2004). Zona birefringence intensity is higher in conception cycles(Shen 2005)

The multilaminar structure of the ZP revealed by polarization microscopy is directly linked to the paracrystalline network structure of the zona which is formed during the follicular maturation by the oocyte.

So a high birefringence of the inner zona layer might indicate an optimal formation of the ordered structure during oocyte maturation. HZB oocytes can have better conditions during follicular growth and maturation compared with a LZB oocyte with unordered zona structure. Regular structural integrity of ZP may reflect an optimal cytoplasmic potential of an oocyte and its various cellular and molecular structures

Non-invasive Embryo Assessment Approaches Possible Targets to Use for Testing

Morphology	☐ Birefringence (SpindleView) ☐ EmbryoScope/Monitoring System
Metabolic Activity	☐ Pyruvate/Glucose uptake ☐ Amino acids* ☐ Oxygen consumption (Respirometry)
Constituents	☐ Genome ☐ Transcriptome (cumulus cells) ☐ Proteome* ☐ Metabolome*
Secreted Factors	☐ PAF ☐ HLAg ☐ “Secretome”*

Nagy; RBMo, 2008: Symposium: innovative techniques in human embryo viability assessment.

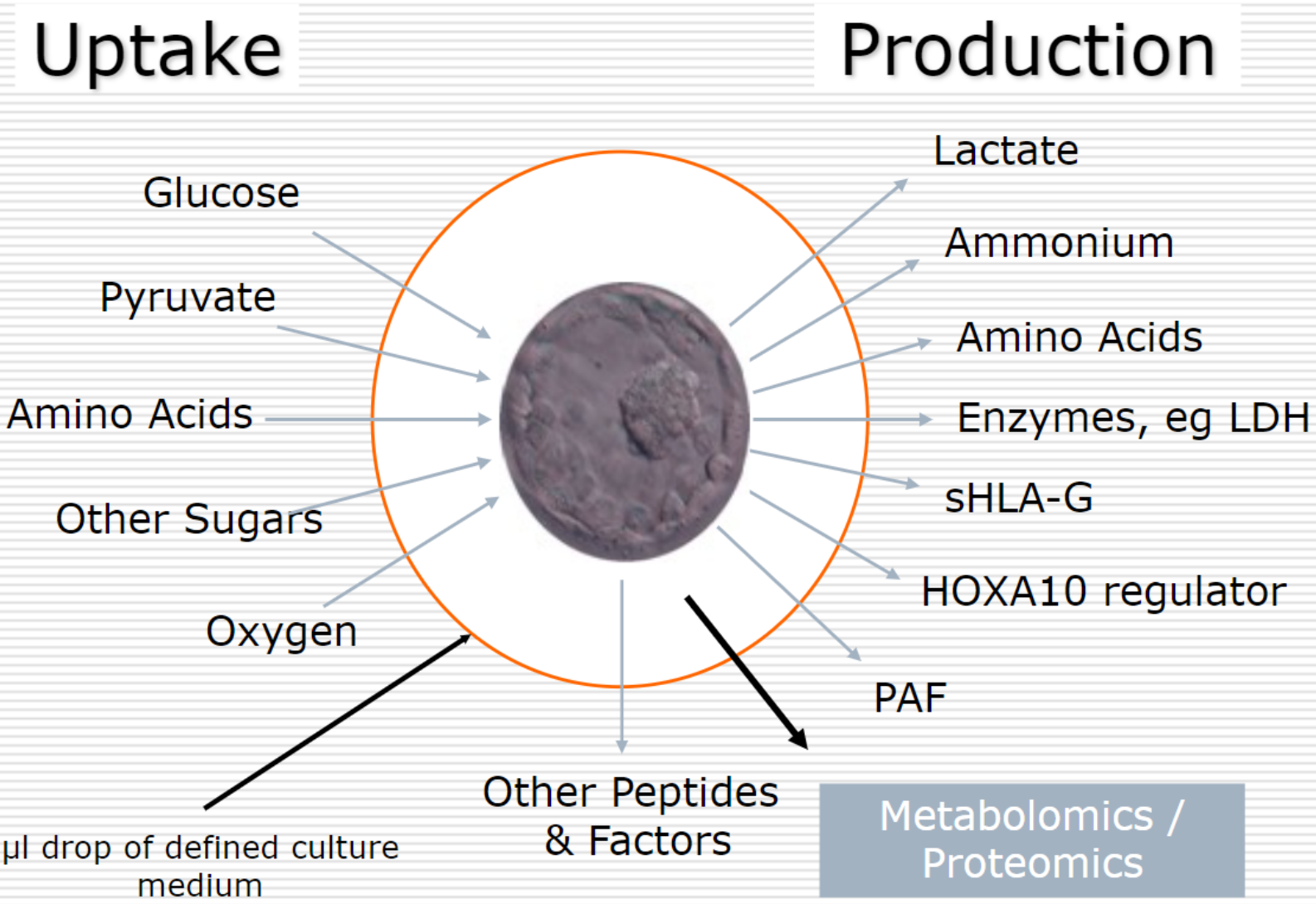

Modified from: Gardner and Leese (1993) Assessment of embryo metabolism and viability. In: Handbook of In Vitro Fertilization. Eds Trounson & Gardner CRC Press. pp195-211.

More objective biomarkers for gamete/embryo selection??

Measurement of specific molecules secreted within the culture environment of the embryo,Objective biomarker for gamete/embryo viability?

Table 1. Summary of Emerging Biomarkers for Non-Invasive Assessment of Embryo Viability in Assisted Reproduction

	Invasive *vs.* Non-invasive	Associated with embryo viability	Predicts embryo viability in blinded analysis
Pyruvate	NI	+	NR
Glucose	NI	+	NR
Lactate	NI	+	NR
Amino acids	NI	+	NR
HLA-G	NI	+	+
Oxygen	NI	—	NR
Genomics	I	+	NR
Transcriptomics	I	+	NR
Proteomics	NI	+	NR
Metabolomics	NI	+	+

NI: non-invasive; I: invasive; NR: not reported; —: no, +: yes.

These investigational approaches are all based on the hypothesis that ″an embryo that results in a pregnancy alters its environment differently compared to a non-viable embryo ‶

Aydıner et al., Cur.Mol.Med. 2010

'OMICS' Technologies

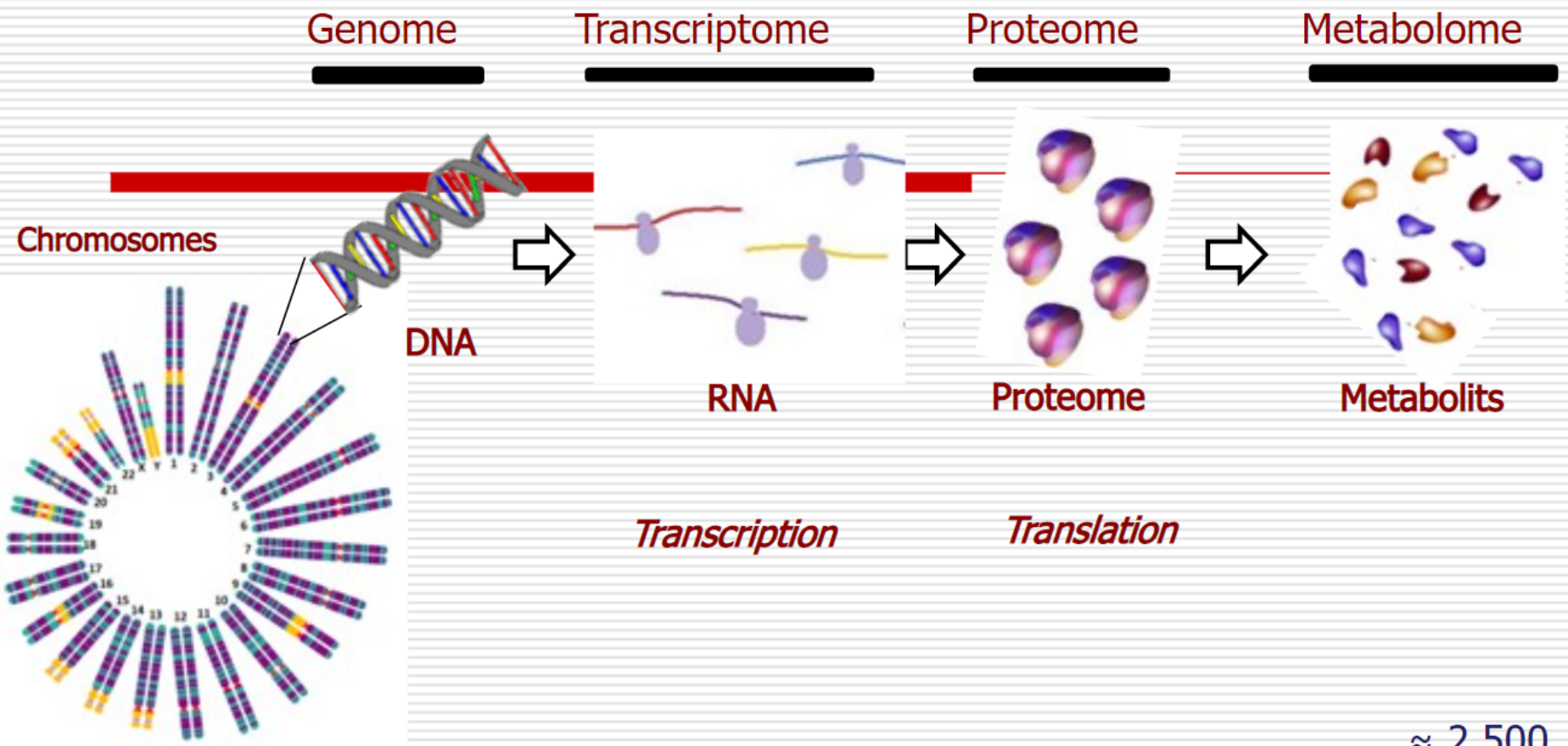

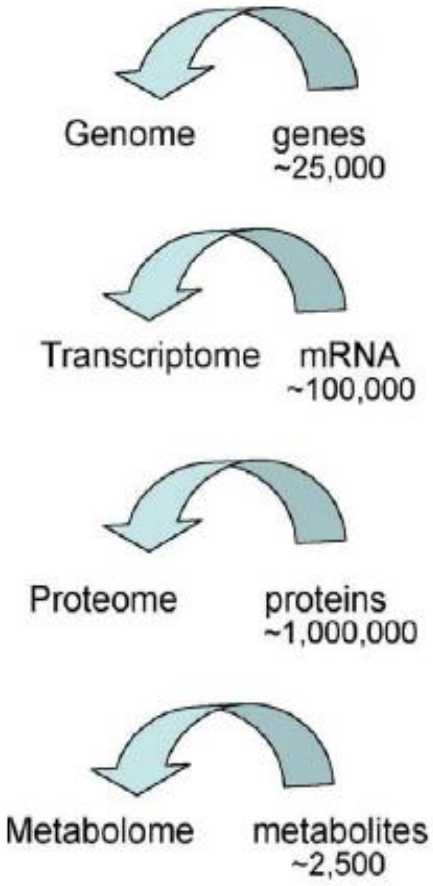

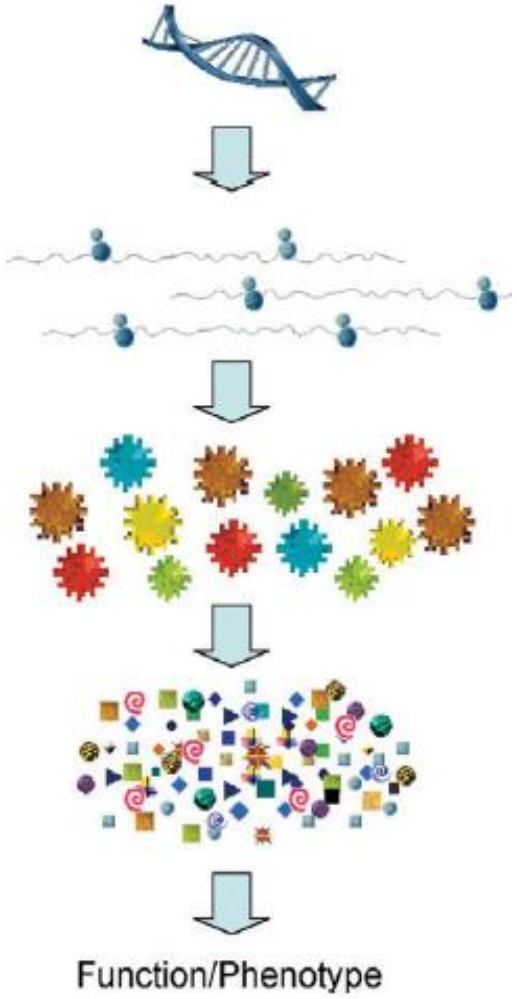

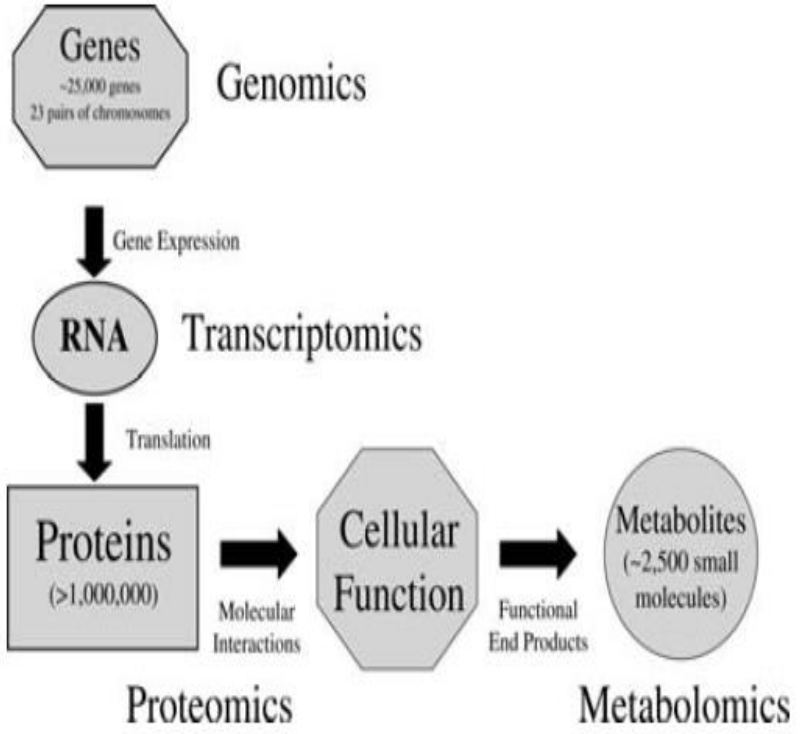

Nagy et al., RBM Online 2008

Katz et al., MHR 2009

OMICS Technologies

- Novel technologies that allow simultaneous profiling of multiple markers (measured from secreted and consumed components within culture medium) of embryonic phenotype

- Genomics (requires embryo biopsy-Invasive)
- Transciptomics (requires embryo biopsy-Invasive)
- Proteomics
- Metabolomics

- Most of the techniques are invasive, technically challenging, and time consuming, and require agents such as radioactive probes or fluorescent dyes, making them unsuitable for assessment of embryo viability in a clinical setting

- Taking into account the complexity and diversity of the human embryo, it would seem reasonable to envisage a combined omics contribution to the characterization of the human embryonic secretome

Genomics

- Studying the DNA constitution/sequence of cells
- DNA determines the sequence of transcripts and is central to protein synthesis and phenotype determination.The existance of genetic determinants for embryo viability is therefore conceivable and could be identified by analysing individual's DNA. However, specific DNA variant sequences associated with increased viability have not been identified.
- In addition the variability in the DNA within a cohort of embryos generated by a given couple will be limited to meiotic recombination. Therefore whether an analysis of embryonic DNA sequence can generate information on embryo viability is still unknown

Transcriptomics

- **Transciptome:** All transcribed elements, regardless of whether they are protein-coding sequences or not
- **Transcriptomics:** Microarray analysis through RNA for investigation of gene expression in oocytes and embryos
- Small RNA molecules such as microRNAs are isolated and processed. Main focus of transcriptomics is directed at protein-encoding RNAs (mRNA)
- Aside from mRNAs,RNA subtypes involved in the maturation process of mRNAs and rRNAs , respectively localized in the nucleus (small nuclear RNAs)and in the nucleolus (small nucleolar RNAs) are important components of transcriptomics
- Proportion of mRNAs in a transcriptome account for only 1-2% of total RNA content in somatic cells

Proteomics

- Entire complement of proteins expressed by a single embryo at a given time is called the embryonic proteome, and it's study is proteomics. Since this is related with gene expression, it can give insight into cellular health and viability.
- The secretome is the subset of proteins that are exported from the cell in which build up the culture environment
- Changes in protein profiles were detected between embryos of different developmental stages, as well as between embryos that progressed versus those arrested. (Katz-Jaffe 2008)
- Despite new advances in proteomic techs.,knowledge of the proteome of the mammalian preimplantation embryo remains limited. The combined effect of limited template, low protein expression and the lack of sensitivity of proteomic platforms are the main hurdles

Proteomic Technologies

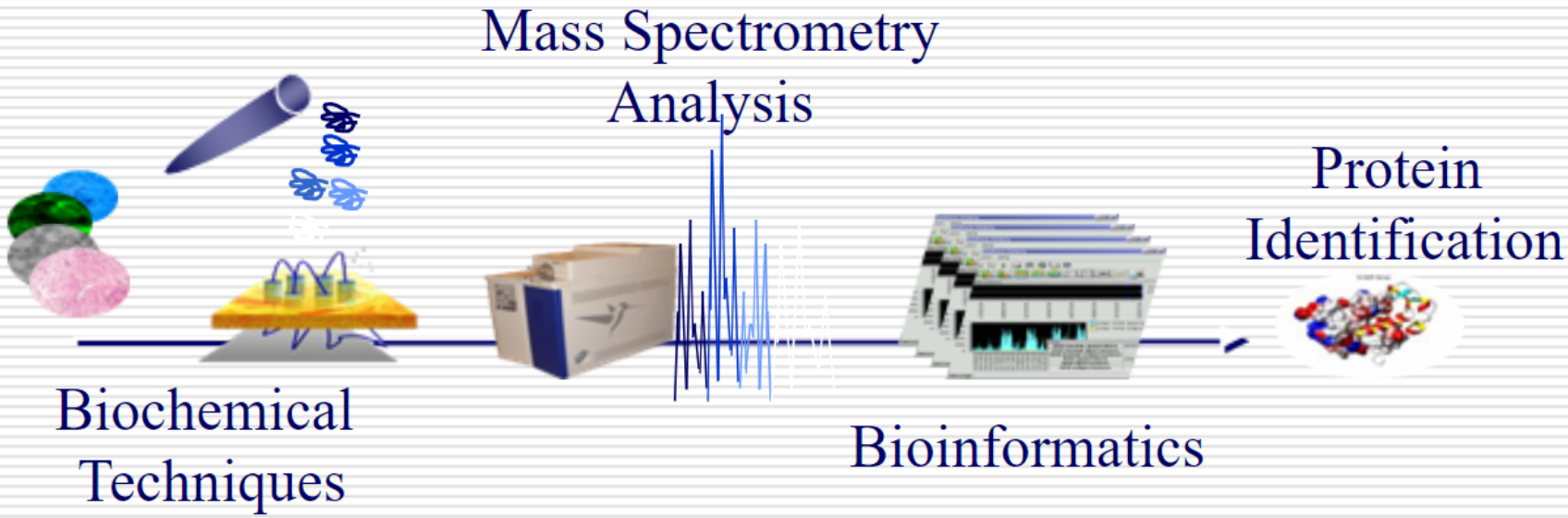

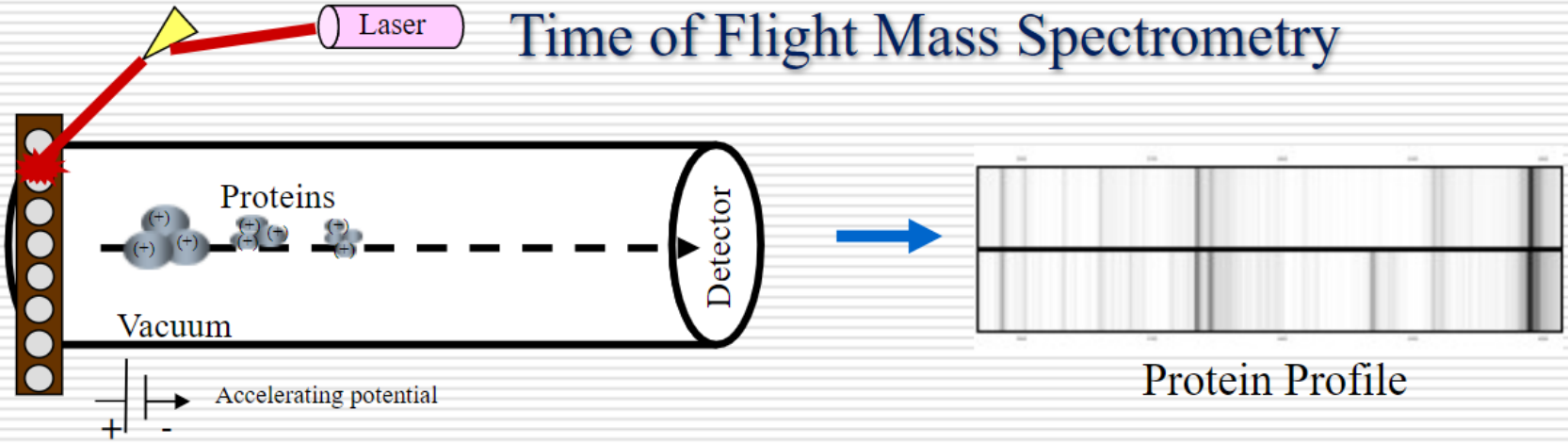

Soluble Human Leukocyte Antigen-G(sHLA-G)

- HLA-G molecule may play a role in immune tolerance in pregnancy, being expressed in the plasenta . Both membrane and soluble forms (sHLA-G) are identified, possibilly sHLA-G having the role of protecting the developing embryo from the maternal immune system. This led the detection of HLA-G mRNA expression in oocytes & embryos, and a positive correlation was found between embryonic HLA-G mRNA expression and pregnancy (Jurisicova 1996)
- It's suggested that there's a positive correlation between sHLA-G in the culture media (measured by ELISA) and increased embryo viability and improved pregnancy rates
- Vercammen 2008, HR Update Meta-Analysis of 11 studies/1813 patients

  sHLA-G in embryo culture supernatants is moderately helpful to predict the ability to achieve a pregnancy in women undergoing infertility treatment. If the embryos are of good quality, however, sHLA-G has a much better diagnostic performance. Our findings underscore the need to address the critically important issues related to single-embryo transfer, single culture condition, and sHLA-G detection threshold

- **Leptin**
- Secretion of leptin, a small pleitropic peptide linked to food consumption and energy balance, measured in the spent embryo culture medium had shown a positive correlation with blastocyst development

***Both methods are technicially challenging and not practical for a clinical setting

Blastocentesis’

sampling and analysis of DNA in the blastocoel cavity

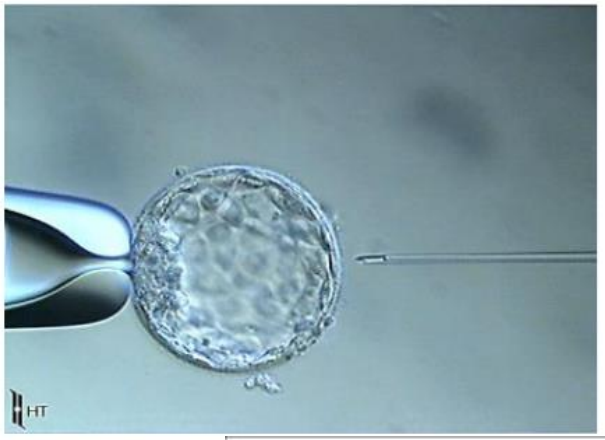

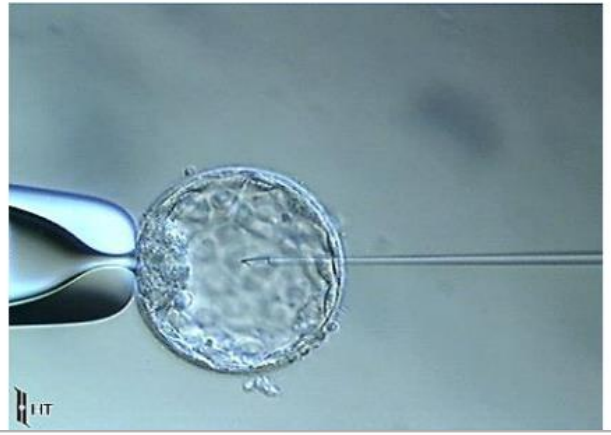

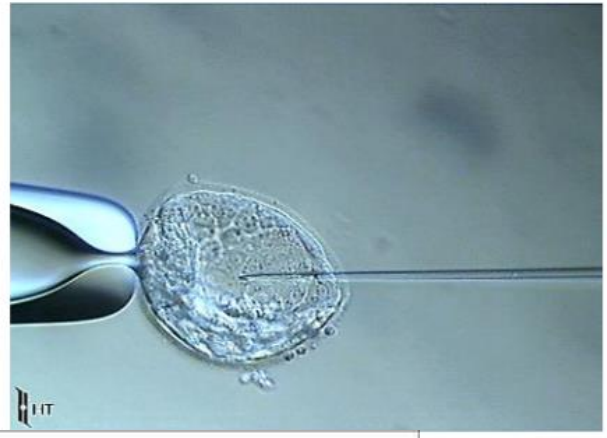

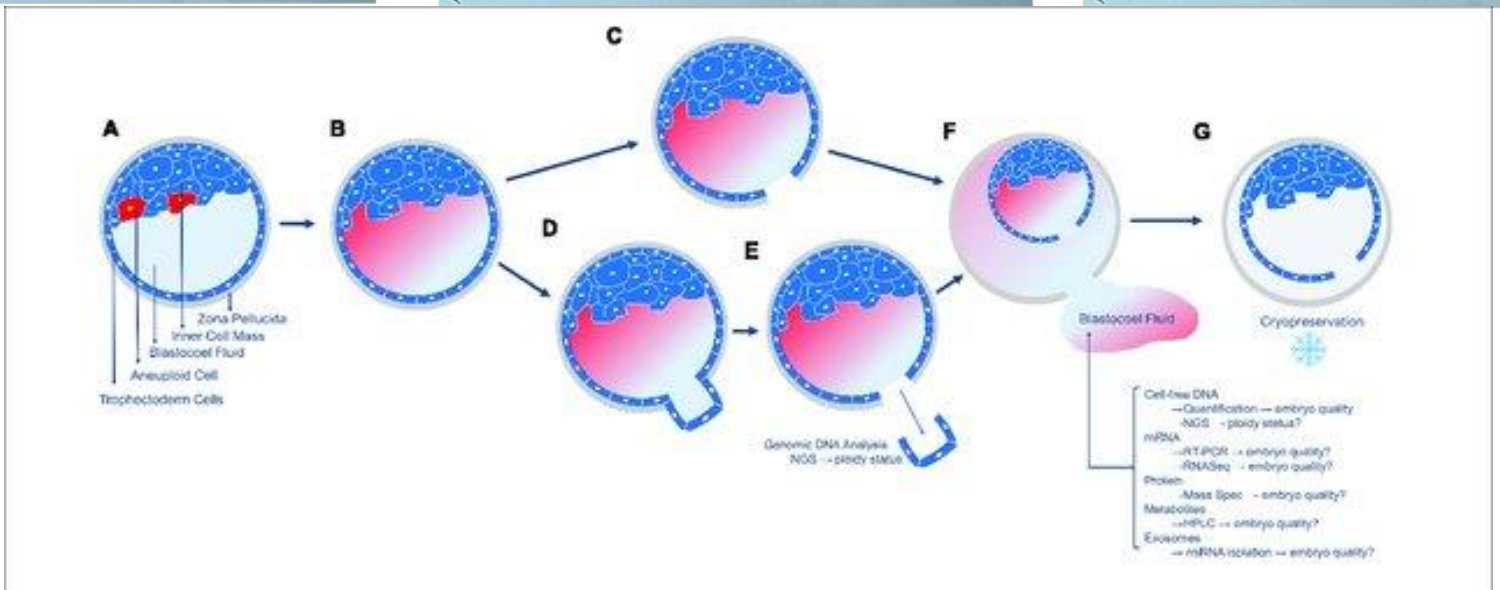

Study	Sample details		Sample handling				Analysis				Concordance (%)		
	Source of BF	Fresh/frozen	Additional manipulations	Day of BF isolation	Volume of isolated BF (estimated)	Handling of isolated BF	Volume used for amplification	WGA method	Amplification rate (%)	Cytogenetic method	Overall ploidy (aneuploid or euploid)	Full karyotype	Per single chromosome
Palini *et al.* (2013)	5 embryos from couples undergoing IVF	Fresh	None	5	0.3–0.5 nl	Transferred to 4 µl mmol/l Tris-HCl, 0.1 mmol/l EDTA sol and stored at −20°C	0.3–0.5 nl	REPLI-g Mini Kit (Qiagen)	80	aCGH (24Sure, Illumina)	–	–	–
Gianaroli *et al.* (2014)	51 supernumerary embryos from couples undergoing PGT-A	Fresh	PB biopsy; assisted hatching; BM biopsy	Not specified	~1 µl	Transferred to empty tube, spun and stored at −80°C	~1 µl	SurePlex (Illumina)	77	aCGH (24Sure, Illumina)	PB: 93 BM: 100 TE: 97	PB: 74 BM: 90 TE: 82	PB: 94 BM: 94 TE: 97
Magli *et al.* (2016)	116 supernumerary embryos from couples undergoing PGT	Fresh	PB biopsy; assisted hatching; BM biopsy	5/6	0.01 µl	Transferred to empty tube, spun and stored at −80°C	0.01 µl	SurePlex (Illumina)	82	aCGH (24Sure, Illumina)	PB: 94 BM: 95 TE: 97	PB: 74 BM: 81 TE: 81	PB: 98 BM: 98 TE: 98
Tobler *et al.* (2015)	96 embryos unsuitable for clinical treatment	Cryopreserved at cleavage or blastocyst stage	BM biopsy; Freeze-thaw	Not specified	~1 µl	Transferred to 2.5 µl PBS and centrifuged at high speed for 3 min	–	SurePlex (Illumina)	63	aCGH (24Sure, Illumina)	WE: 62	WE: 48	–
Tšuiko *et al.* (2018)	16 embryos donated following IVF	Cryopreserved blastocysts	Freeze-thaw	Not specified	~0.01 µl	Transferred to 2.5 µl PBS and immediately amplified	~0.01 µl	PicoPlex (Rubicon Genomics)	87	NGS (VeriSeq, Illumina)	TE: 70 ICM: 70	TE: 40 ICM: 40	–
Capalbo *et al.* (2018)	23 embryos from couples undergoing PGT	Fresh	None	5/6/7	Aspirated until cavity 10% of its original volume	Transferred to 5 µl HEPES buffered medium. Stored at −80°C	–	SurePlex (Illumina)	35	NGS (VeriSeq, Illumina)	TE: 75	TE: 38	–
Magli *et al.* (2018)	256 embryos from couples undergoing PGT-A	Fresh	None	Not specified	~1 µl	Transferred to 1 µl PBS on cold racks and spun immediately. Stored at −80°C	~1 µl	SurePlex (Illumina)	71	aCGH (24Sure, Illumina)	TE: 94	TE: 66	TE: 96

Details of the major studies to date performing PGT-A on BF-DNA, specifically, their rates of amplification achieved and reported karyotype concordance with cells of the embryo. PB: polar bodies; WE: whole embryo; BM: blastomere; TE, trophectoderm; –, information not provided by the study.

From: Minimally Invasive Cell-Free Human Embryo Aneuploidy Testing (miPGT-A) Utilizing Combined Spent Embryo Culture Medium and Blastocoel Fluid – Towards Development of a Clinical Assay

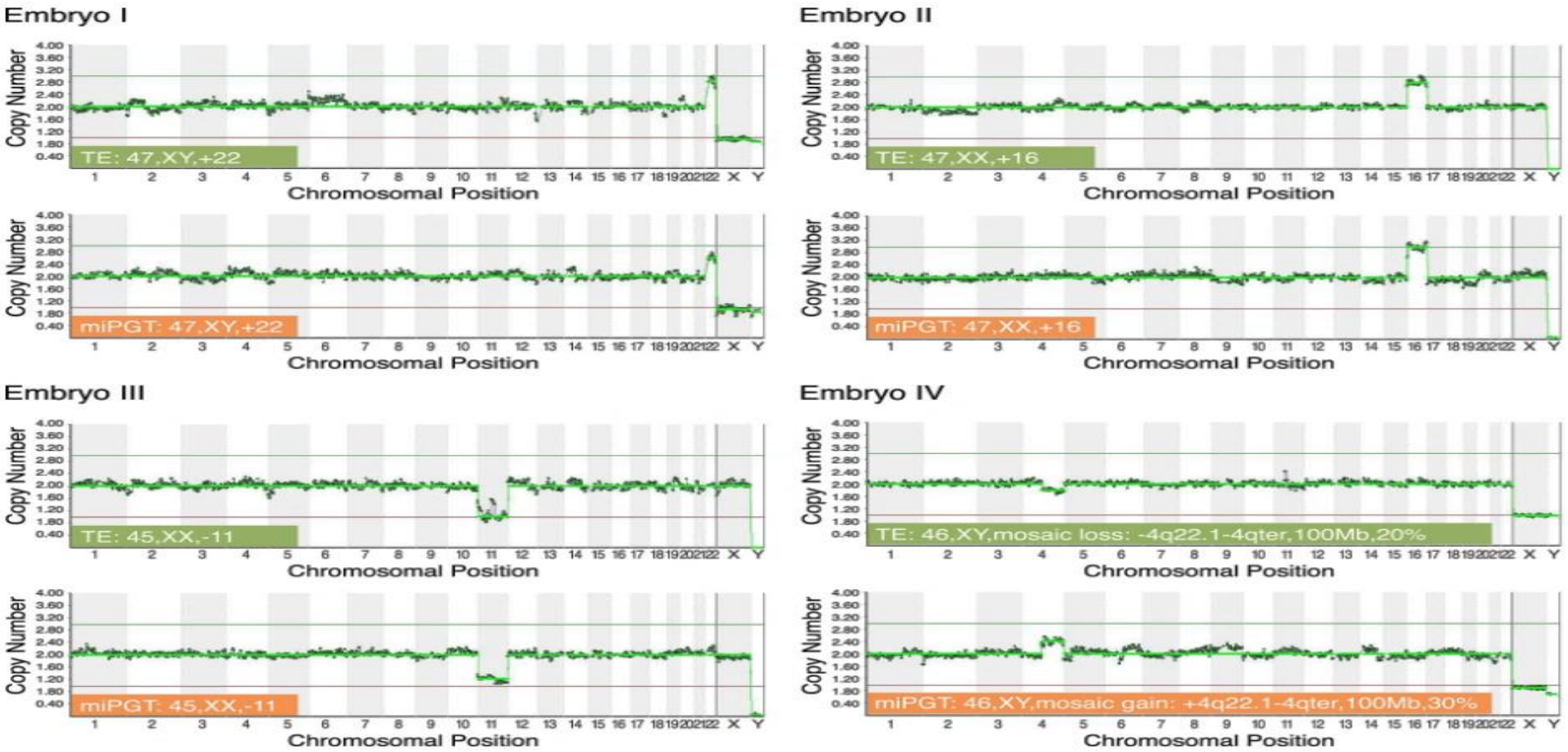

Four examples of NGS results representing 24 chromosome copy number plots from TE biopsy and corresponding miPGT samples with concordant results for aneuploidy in three examples and mosaic-complementary in terms of loss versus gain on chromosome 4q (segmental chromosomal mosaicism) in the fourth embryo.

Kuznyetsov, et al Sci Rep 10, 7244 (2020).

From: Minimally Invasive Cell-Free Human Embryo Aneuploidy Testing (miPGT-A) Utilizing Combined Spent Embryo Culture Medium and Blastocoel Fluid –Towards Development of a Clinical Assay

Embryo number	TE biopsy	miPGT, ≥BB
Euploid-euploid		
1	XX; normal	XX; normal
2	XX; normal	XX; normal
3	XX; normal	XX; normal
4	XX; normal	XX; normal
5	XX; normal	XX; normal
6	XX; normal	XX; normal
7	XX; normal	XX; normal
8	XY; normal	XY; normal
9	XX; normal	XX; normal
10	XX; normal	XX; normal
11	XY; normal	XY; normal
12	XY; normal	XY; normal
13	XX; normal	XX; normal
14	XY; normal	XY; normal
15	XY; normal	XY; normal
16	XY; normal	XY; normal
17	XY; normal	XY; normal
18	XX; normal	XX; normal
19	XY; normal	XY; normal
20	XY; normal	XY; normal
21	XX; normal	XX; normal
22	XY; normal	XY; normal
23	XY; normal	XY; normal
24	XX; normal	XX. normal
25	XY; normal	XY; normal
26	XX; normal	XX; normal
Euploid-mosaic		
27	XY; normal	XY; mosaic −8 (70%)
28	XY; mosaic −9 (30%)	XY; normal
29	XX; mosaic −15 (20%)	XX; normal
30	XX; mosaic: −8p (35%), −9p (35%)	XX; normal
31	XX; normal	XX; mosaic −9 (70%)
Mosaic-mosaic		
32	XY; mosaic −4q (118.6 Mb, 20%)	XY; mosaic +13q21.1 −q 31.3 (34.84 Mb, 60%)
33	XY; mosaic loss: (−4q22.1-q35.2, 100 Mb, 20%)*	XY; mosaic gain: (+4q 22.1-q35.2, 100 Mb, 30%)*
34	XY; mosaic: +8q (50%), −5q15-q35.3 (88MB, 35%)	XY; mosaic −3 (70%)
35	XY; mosaic −16 (60%)	XY; mosaic −17 (−70%)
36	XX; mosaic: +8 (50%), +19 (50%)	XX; mosaic: −17 (30%)
37	XX; mosaic: −22 (60%)	XX; mosaic: −22 (70%)
Segmental aneuploid-euploid		
38	XX; normal	XX; −5q23.3-q35.3 (51.71 Mb)
Aneuploid-aneuploid		
39	XX; −14	XX; −14
40	XX; −15	XX; −15
41	XY; +16, +21	XY; +16, +21
42	XX; +16	XX; +16
43	XY; −7, −15, −18	XY; −7, −15, −18
44	XX; −22	XX; −22
45	XX; −13	XX; −13
46	XY; +16	XY; +16
47	XY; −7	XY; −7
48	XY; +21	XY; +21
Embryo number	TE biopsy	miPGT, <BB

Kuznyetsov, et al Sci Rep 10, 7244 (2020).

Euploid-euploid		
1	XX; normal	XX; normal
2	XY; normal	XY; normal
3	XY; normal	XY; normal
4	XX; normal	XX; normal
5	XY; normal	XY; normal
6	XX; normal	XX; normal
7	XX; normal	XX; normal
8	XX; normal	XX; normal
9	XY; normal	XY; normal
10	XX; normal	XX; normal
11	XX; normal	XX; normal
12	XY; normal	XY; normal
13	XY; normal	XY; normal
14	XX; normal	XX; normal
15	XY; normal	XY; normal
16	XX; normal	XX; normal
17	XX; normal	XX; normal
Euploid-mosaic		
18	XX; mosaic loss: (−3p.26.3 ± p25.2, 12 Mb, 35%)	XX; normal
19	XX; mosaic gain: +12p13.33-q23.3 (105.5 Mb, 45%)	XX; normal
20	XY; mosaic +16p (40%)	XY; normal
21	XX; mosaic −8 (40%)	XX; normal
Mosaic-mosaic		
22	XY; mosaic +6q22.1-q.25.2 (38.5 Mb, 45%), mosaic −15 (50%)	XY; mosaic −8 (50%)
23	XY; mosaic loss: −3q26.31-q29 (24.4 Mb, 65%)	XY; mosaic loss: −3q26.31-q29 (24.4 Mb, 65%)
24	XX; mosaic: +4 (30%), +5 (30%), +8 (30%), +10 (50%)	XX; mosaic: +5 (40%), +10 (40%)
25	XY; mosaic + 14q11.2-q32.33, 84.69 Mb, 65%*	XY; mosaic −14q11.2-q32.33, 84.69 Mb, 60%*
26	XY; mosaic +4 (40%)	XY; mosaic +4 (50%)
Complex Aneuploid-mosaic		
27	XX; −18	XX; mosaic −18q12.2-q23 (43.75 Mb, 40%)
Aneuploid-aneuploid		
28	XY; −5, −13	XY; −5, −13
29	XX; +19	XX; +1919
30	XY; +10, −11, −20	XY; +10, −11, −20
31	XY; +11, −16, +22	XY; +9, +11, −16, +22
32	XX; +22	XX; +22
33	XX; +13, +19, −21	XX; +13, +19, −21
34	XY; +11, mosaic gain: +10q23.31-26.3 (44.26MB, 50%)	XY; +10, +11, +16
35	XX; −3p26.3-p22.1 (39, 8 Mb)	XX; −3p26.3-p22.1 (39, 8 Mb)
36	XY; −17, +21, mosaic: +1p31.1-p21.1 (39 Mb, 30%)	XY; −17, +21
37	XY; −19	XY; −19
38	XY; −4, −8, +9, +18	XY; −4, −8, +9, +18
39	XY; +22	XY; +22
40	XX; −11	XX; −11
41	XY; −22	XY; −22
42	XY; +16	XY; +16

*Mosaic-complementary in terms of chromosomal gain versus loss between TE biopsy and miPGT samples.

Blastocysts were grouped based on their static morphology in good if graded as ≥1/2 BB, or moderate/low if graded <1/2BB.

Kuznyetsov, et al Sci Rep 10, 7244 (2020).

Microfluidics

Microfluidic technology provides a unique means of interfacing known analytical methods for embryo developmental physiology and molecular phenotypes in real time

Fluid handling systems (made of glass or polymer; PDMS) incorporating structural flow features (eg. branced or unbranched channels) that exploit the unique physical differences between macro- and micro scale fluids. They utilize rectilinear fluid channels width >100µm with respect to height >10µm and up to centimetres long. (10µl of culture medium,and 10 mm long would hold 10nL. Volume:cross section area x lengthFor ex. a human blastocyst is 175-225 µm in diameter, equating to 5 nL in volume capacity

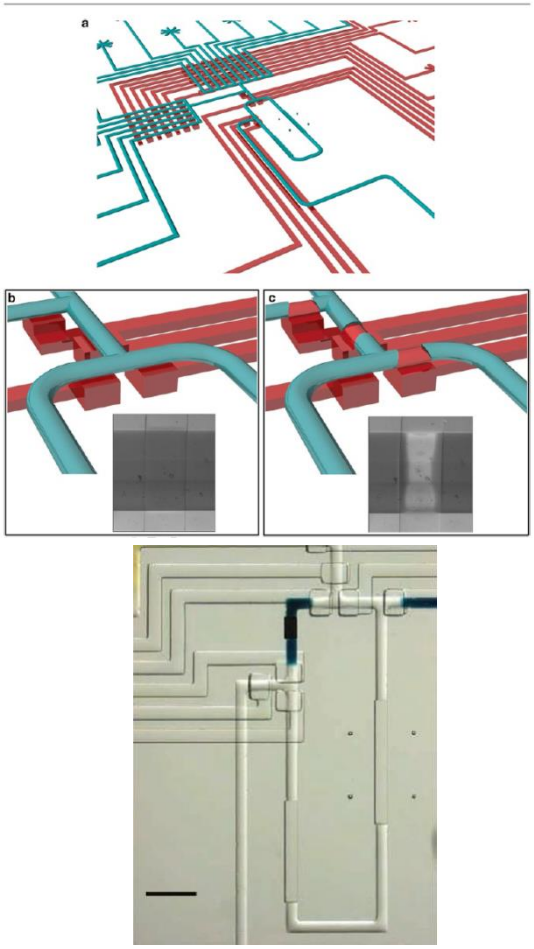

Aim: Ideal device could be an active, continuous culture platform with integrated time-lapse imaging and metabolomic or secretomic endpoints, Providing real-time physiological outputs as the embryo develops, as well as sampling for interface with more detailed molecular analysis.

Details to be solved before using these devices in clinical practice,

- Suitability of microfluidics for analysis of oocyte & embryo morphology, integration of time-lapse monitorization
- Adaptation of combined omics technology for oocytes & embryos

To produce devices with more automation and less user intervention to systematize assisted reproductive technology laboratories

Gardner et al., Human Gametes and Preimplantion Embryos. Assessment and Diagnosis, 2013

Non-invasive, label-free optical analysis to detect aneuploidy within the inner cell mass of the preimplantation embryo

C.Y. Tan O-083

Hyperspectral imaging

- Many molecules have the capacity for autofluorescence, e.g. NADH, FAD, retinoids, elastin and collagen

- Hyperspectral imaging is able to record many spectra in parallel

FAD, flavin adenine dinucleotide;
NADH, reduced nicotinamide adenine dinucleotide.

Gosnell ME, et al. Sci Reports. 2016;6:23453.

Oxidative phosphorylation[1]

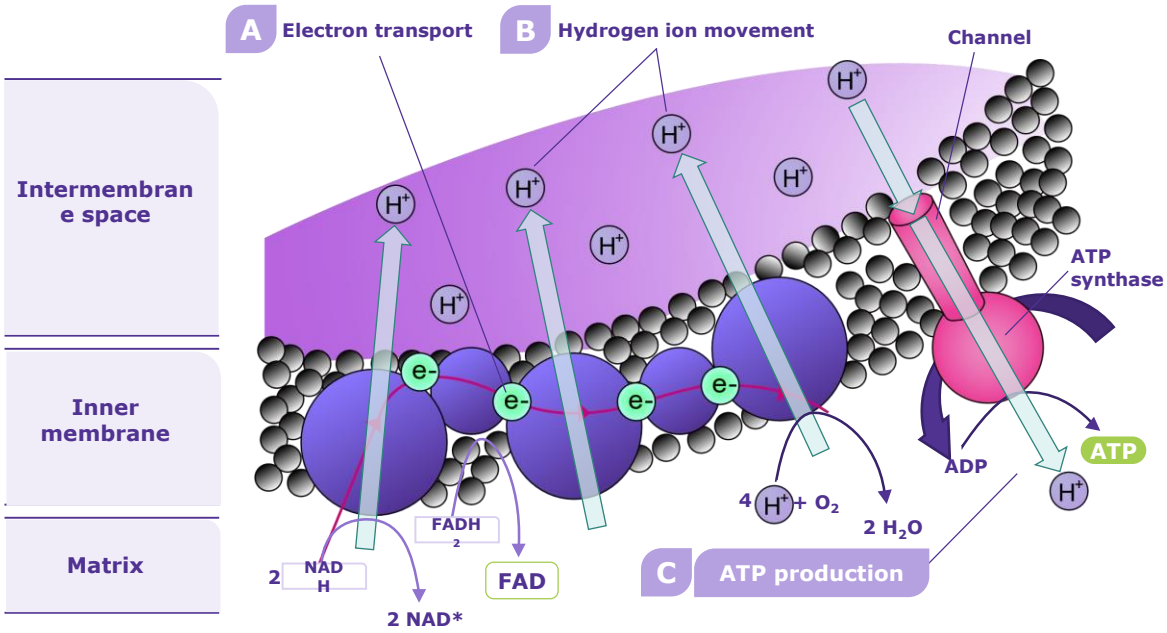

Aneuploid cells have an altered metabolism[2]

ATP, adenosine triphosphate; $FADH_2$, reduced flavin adenine dinucleotide; NAD, nicotinamide adenine dinucleotide.

1. Electron transport chain + oxidative phosphorylation. Available from: https://ckyscience.com/topic-8-2-electron-transport-chain-oxidative-phosp-t386.html. Accessed August 2021.
2. Tan CY, et al. Presented at ESHRE 2021; O-083.

Human fibroblasts

Optical redox ratio[1] = $\frac{\text{FAD}}{\text{NAD(P)H + FAD}}$

Comparison between euploid and aneuploid cells:[2]

NADH ↑

FAD ↓

(i.e., low cell metabolism)

→ $\frac{\text{FAD}}{\text{NAD(P)H + FAD}}$ = Optical redox ratio in aneuploid cells ↑

Aneuploidy leads to lower cellular metabolism in human fibroblast cells, reflected by the optical redox ratio[2]

1. Chance B, et al. J Biol Chem. 1979;254:4764-71.
2. Tan CY, et al. Presented at ESHRE 2021; O-083.

Generation of aneuploid mouse blastocysts[1]

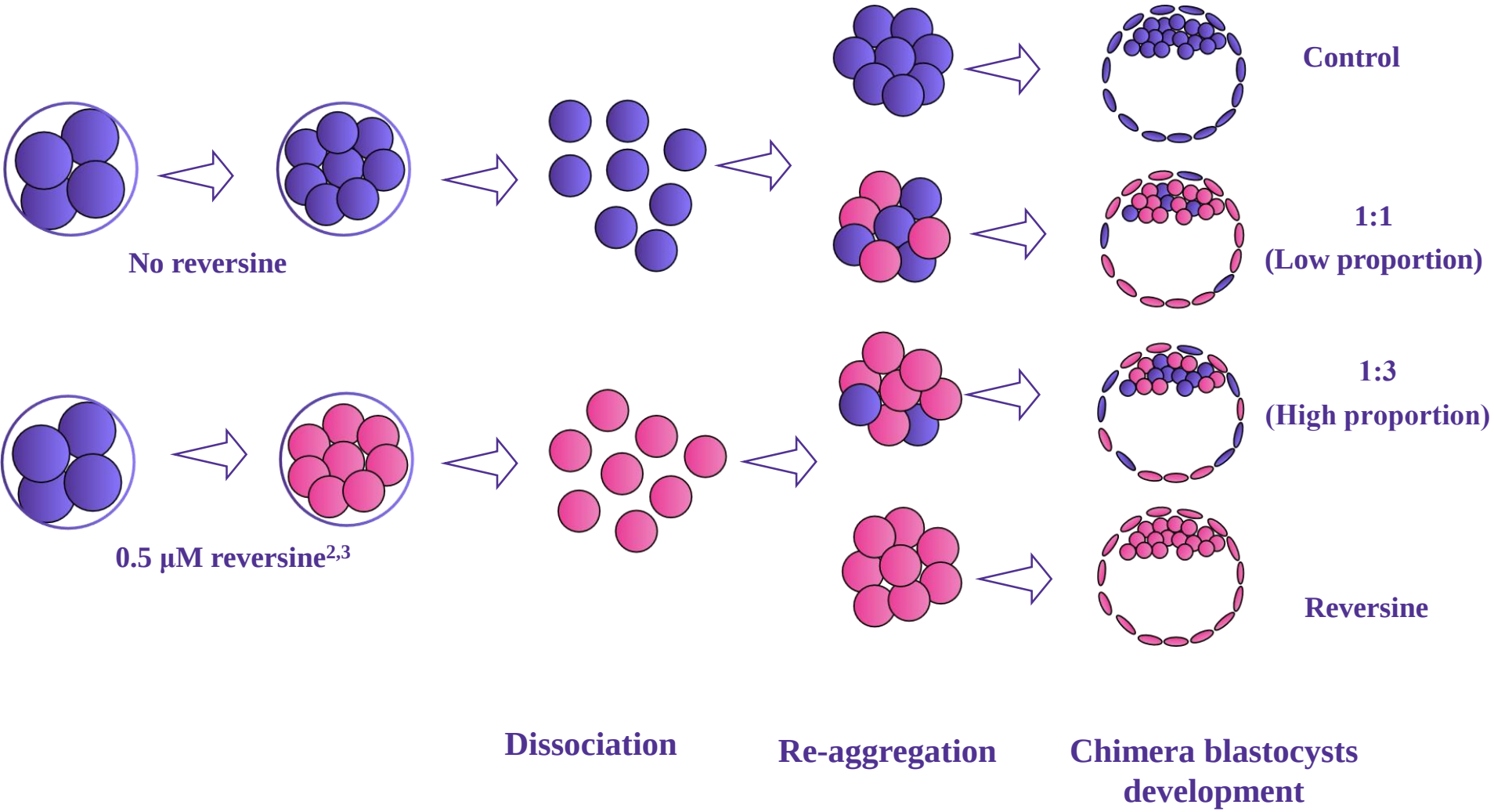

1. Tan CY, et al. Presented at ESHRE 2021; O-083.
2. Santaguida S, et al. J Cell Biol. 2010;190:73-87.
3. Bolton H, et al. Nat Commun. 2016;7:11165.

Mouse model

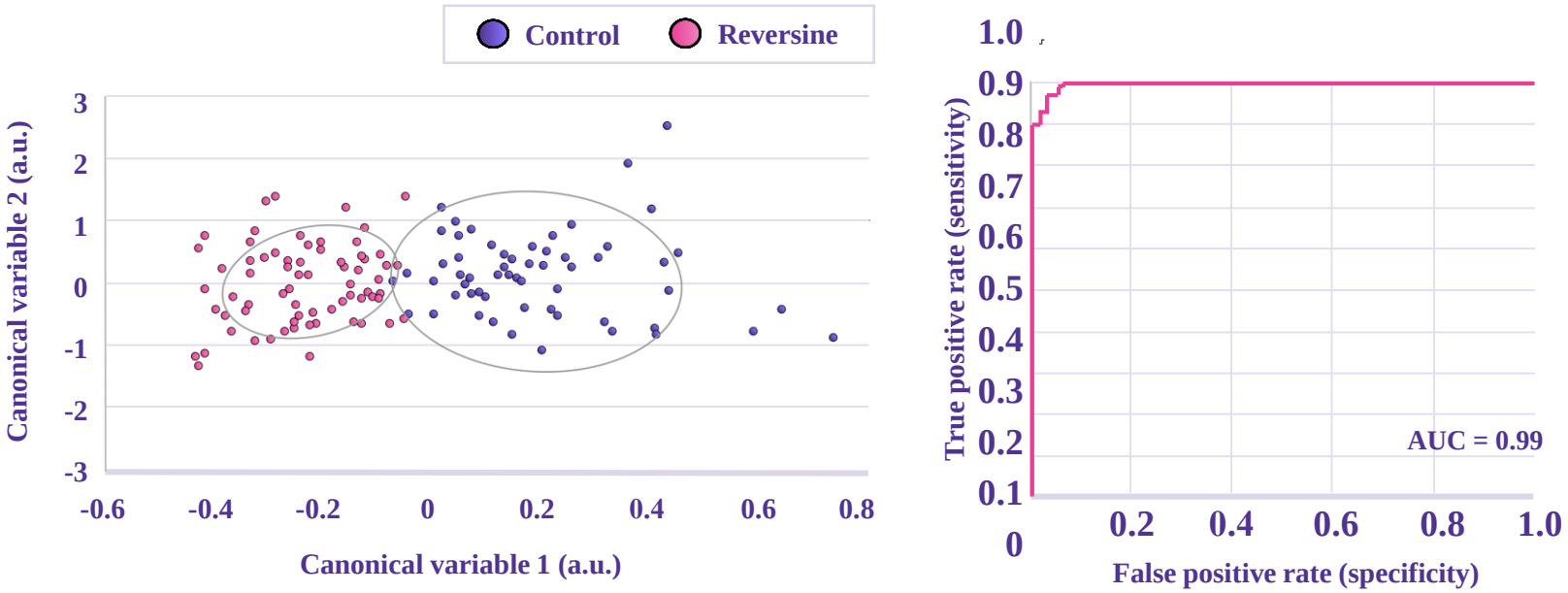

a.u., arbitrary unit; AUC, area under the curve.

Tan CY, et al. Presented at ESHRE 2021; O-083.

FAD decreases in aneuploid ICM

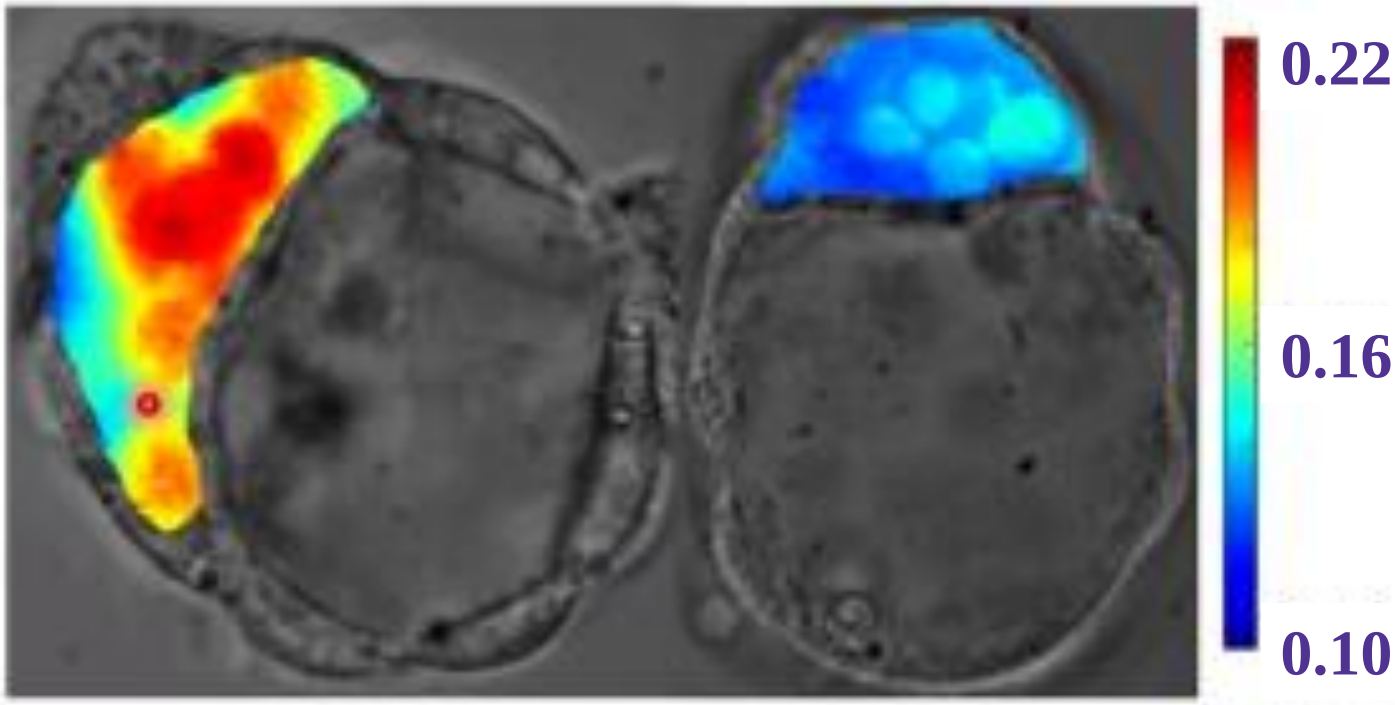

ICM, inner cell mass.

Control **Reversine**

Reversine-induced aneuploidy in mouse chimera blastocysts leads to altered levels of endogenous fluorophores

Tan CY, et al. Presented at ESHRE 2021; O-083.

Mouse model

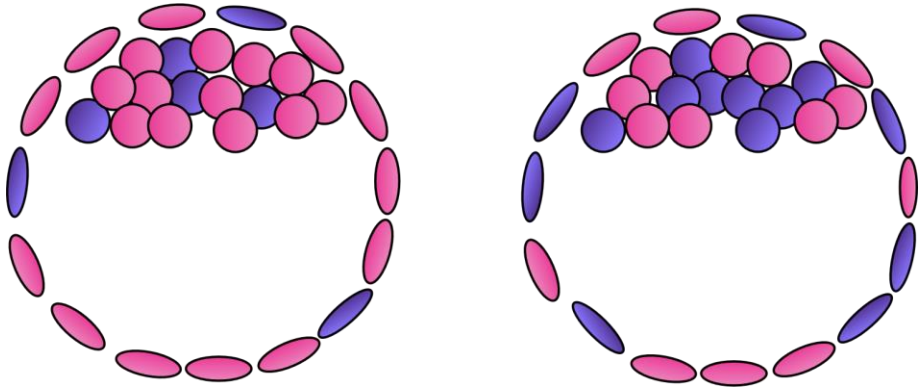

1:3 and 1:1 mouse chimera blastocysts

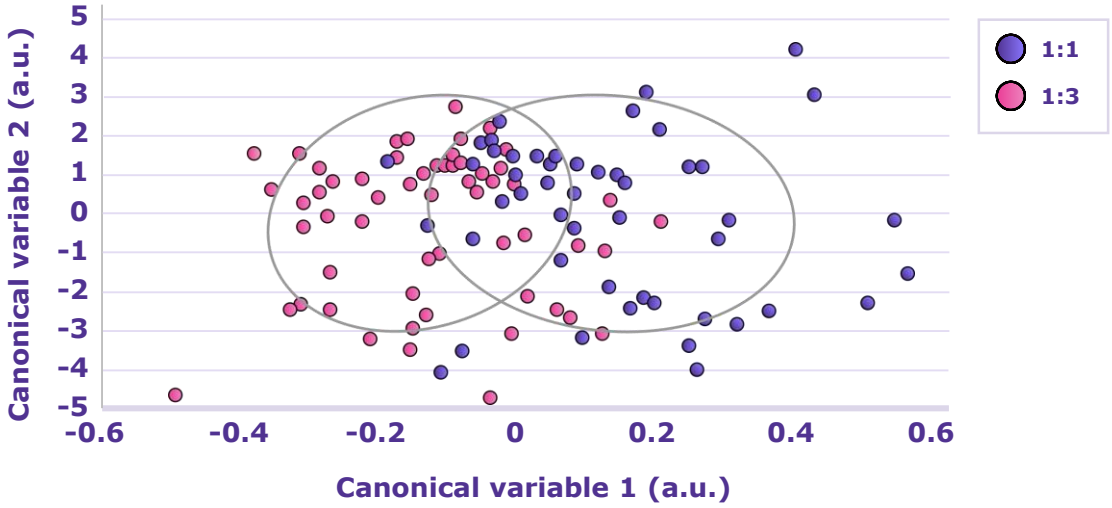

Tan CY, et al. Presented at ESHRE 2021; O-083.

Conclusion

- Hyperspectral imaging allows a distinction between euploid and aneuploid mouse embryos
- Aneuploidy results in altered metabolism
- Hyperspectral imaging does not have any negative effect on mouse embryo quality and offspring health

Tan CY, et al. Presented at ESHRE 2021; O-083.

Computer vision to distinguish between euploid and aneuploid embryos.
A novel artificial intelligence approach to measure cell division activity associated with chromosomal status

L. Bori O-084

Computer vision can distinguish between euploid and aneuploid embryos.
A novel artificial intelligence approach to measure cell division activity associated with chromosomal status

Measurement of blastomere circumferences as a proxy for cell activity using computer vision technology

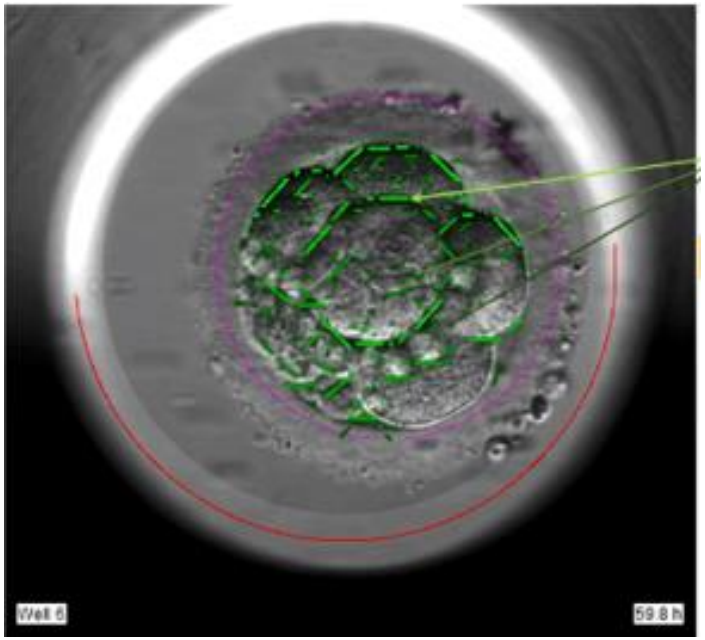

Brightness of green stain indicates score

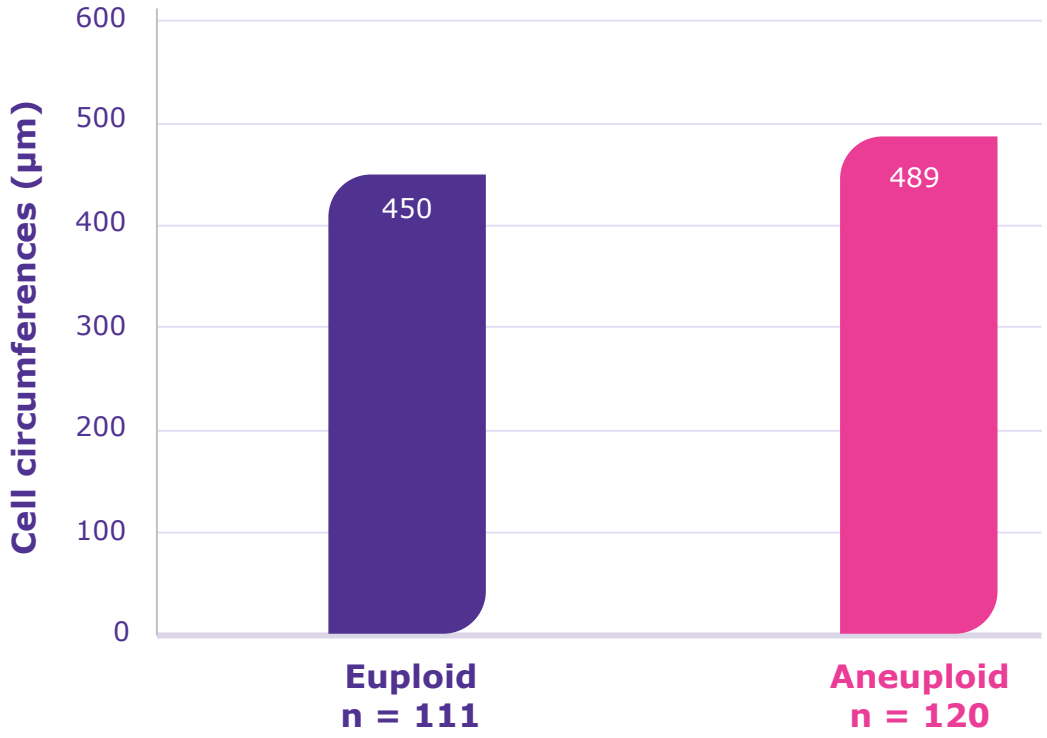

Cell circumferences are larger in aneuploid cells

Bori L, et al. Presented at ESHRE 2021; O-084.

Summary

- Aneuploid embryos blastulate later, possibly due to higher cell activity
- Computer model can measure circumferences precisely
- Aneuploid cells have larger circumferences overall
- Distinction between euploid and aneuploid embryos with 73% accuracy

Bori L, et al. Presented at ESHRE 2021; O-084.

Metabolic imaging of cumulus cells to predict embryo implantation potential

M. Venturas O-172

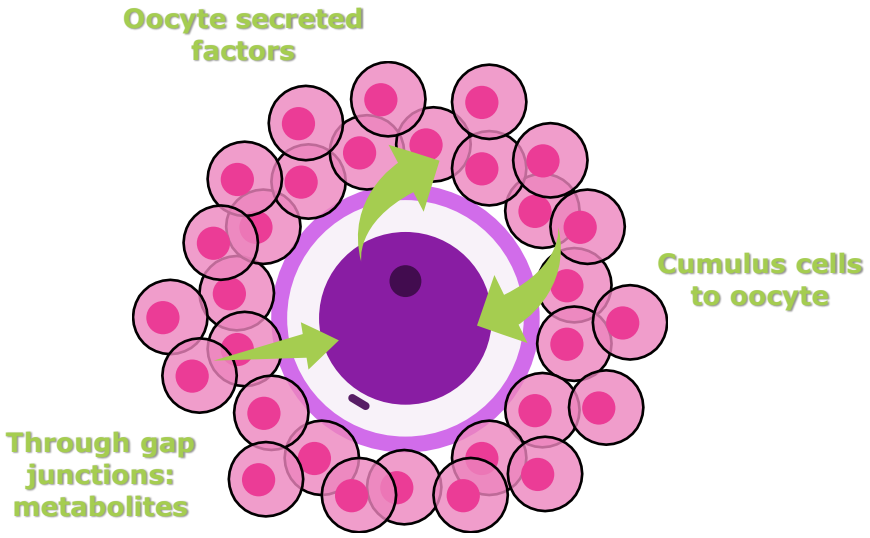

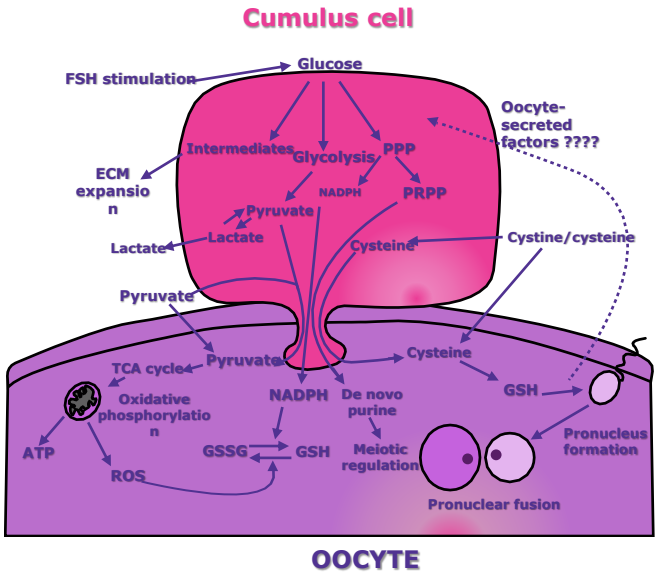

ECM, extracellular matrix; FSH, follicle-stimulating hormone; GSH, glutathione; GSSG, glutathione disulfide; NADPH, nicotinamide adenine dinucleotide phosphate; PPP, pentose phosphate pathway; PRPP, phosphoribosyl pyrophosphate; ROS, reactive oxygen species; TCA, tricarboxylic acid.

Communication between cumulus cells and oocytes

Sutton ML, et al. Hum Reprod Update. 2003;9:35-48.

Fluorescence lifetime imaging microscopy (FLIM)

- The method exploits autofluorescence of cellular co-enzymes NADH and FAD+
- NADH and FAD+ used for quantitative measurements of metabolic state of cells

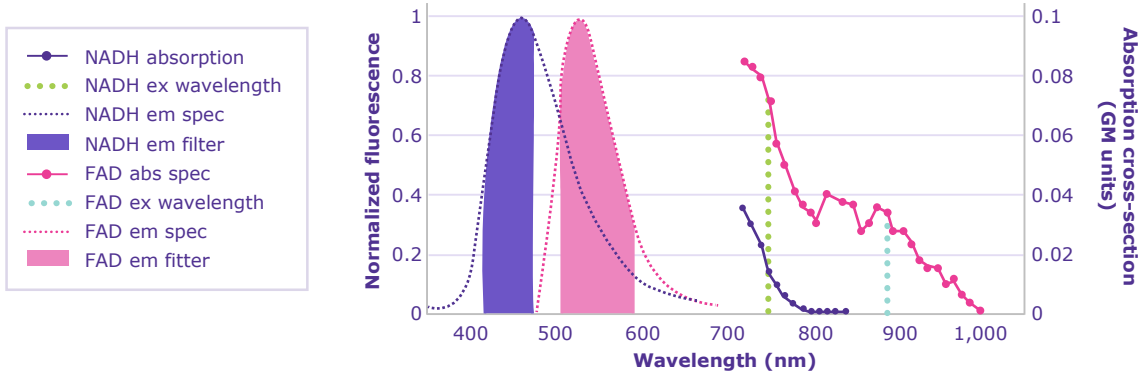

G-M, Goeppert–Mayer.

- The following can be measured by FLIM: providing 4 parameters
  - The time span of autofluorescence: short or long lifetime
  - Free and bound molecules: fraction engaged
  - Optical redox ratio NADH/FAD+: intensity

Venturas M, et al. Presented at ESHRE 2021; O-172.

Conclusions

- **Morphological markers**

Traditional embryo assessment is challenged by different factors, ie, low efficiency/ higly subjective/ predictive value limited!

**BUT still remain to be the solely method of choice, and evidence based !!

- **New objective biomarkers for oocyte and embryo selection**

1. Most likely to be used in the nearest future?

- Utilization of polarized microscopy, Time-lapse monitoring : morphokinetics can be widely spread out in clinical setting with more prospective randomized proofs. Perhaps a combination of these systems might be considered in the near future?

2. To be used in the future with improvements?

- Combined omics technology integrated into microfluidic devices? More time needed
- AI in future can revolutionized IVF especial for non invasive assessment of preimplantation embryo.

***FAST, EASY-TO-USE ,NON-INVASIVE and COST EFFECTIVE

Many couples are hoping for your miraculous hands